Published by
NIGERIAN SOCIETY OF PHYSICAL SCIENCES
Available online @ https://journal.nsps.org.ng/index.php/jnsps

J. Nig. Soc. Phys. Sci. 8 (2026) 3505

Journal of the Nigerian Society of Physical Sciences

Modeling traffic-light systems: A neutrosophic graph approach

K. Deva[a], K. Siva[b], Gamachu Adugna Ganati[c], Walid Abdelfattah[d,*], Fikadu Tesgera Tolasa[e], Nasir Ali[f], Aseel Smerat[g], A. Mehmood[h]

[a]*Department of Mathematics, Vel Tech High Tech Dr. Rangarajan Dr. Sakunthala Engineering College, Avadi, Chennai 600062, Tamil Nadu, India*
[b]*Department of Mathematics, Vel Tech Multi Tech Dr. Rangarajan Dr. Sakunthala Engineering College, Avadi, Chennai 600062, Tamil Nadu, India*
[c]*Department of Mathematics, Wollega University, Nekemte, Oromia, Ethiopia*
[d]*Humanities and Social Research Center, Northern Border University, Arar, Saudi Arabia*
[e]*Department of Mathematics, Dambi Dollo University, Oromia, Ethiopia*
[f]*Department of Mathematics, COMSATS University Islamabad, Vehari Campus, Pakistan*
[g]*Faculty of Educational Science, Al-Ahliyya Amman University, Amman, Jordan*
[h]*Riphah International University, Islamabad 44000, Pakistan*

Abstract

The coloring of neutrosophic graphs (NGs) is an important concept with extensive real-world applications. This research focuses on chromatic numbers for NGs and their operations. We define the neutrosophic chromatic number based on the α-, β-, and γ-cuts, as well as the strong α-, β-, and γ-cuts, of an NG. Furthermore, a comparative analysis of the proposed neutrosophic chromatic number is performed using the neutrosophic independent vertex set, demonstrating the effectiveness of the proposed approach. Several properties related to the union of NGs are also investigated using the proposed neutrosophic chromatic number. Finally, an illustrative traffic-light case study demonstrates the applicability of the proposed graph-coloring framework. The case study shows how the framework can model uncertain traffic conflicts and determine the minimum number of signal phases required for safe traffic operation. In the illustrative example, the obtained neutrosophic chromatic numbers indicate that the traffic network can be managed using five ($k = 5$) signal phases under the proposed model, illustrating the framework's potential for efficient traffic-light scheduling, the reduction of potential traffic conflicts, and support for intelligent traffic-management decisions under uncertainty.

DOI: 10.46481/jnsps.2026.3505

Keywords: Neutrosophic graph coloring, Chromatic number, Single-valued neutrosophic graph, Traffic-light scheduling, Uncertainty modeling

Article history:
Received: 09 May 2026
Received in revised form: 05 July 2026
Accepted for publication: 20 July 2026
Available online: 10 August 2026

Communicated by: B. J. Falaye

1. Introduction

The mathematical discipline of graph theory studies the connections between entities, represented by nodes, and the relationships between them, indicated by edges. Lotfi Zadeh first introduced the concept of a fuzzy set ($\mathcal{FS}$) in 1965, which is a generalization of a classical set in mathematics. This seminal contribution is detailed in his paper titled Fuzzy Sets [1]. In this paper, Zadeh presented the idea that set membership could be characterized by degrees between 0 and 1, allowing for representing uncertainty. $\mathcal{FS}$ find applications in fields like artificial intelligence, decision-making and control systems, providing a tool to handle imprecision and vagueness in various domains. In 1975, Rosenfeld [2] made significant contributions by intro-

*Corresponding author Tel. No.: +966549438136.
Email address: walid.abdelfattah@nbu.edu.sa (Walid Abdelfattah)

ducing fuzzy graph ($\mathcal{FG}$) theory and several analogs of graph-theoretic principles, marking a groundbreaking exploration in this field. P. Bhattacharya [3] established an inherent link between a fuzzy group and a fuzzy graph, introducing novel aspects such as eccentricity and center while exploring the characteristics of fuzzy graphs in 1987. In 1994, Mordeson and Peng [4] introduced a set of operations for fuzzy graphs. The underlying concept of graph coloring in the field of graph theory involves the allocation of colors to vertices, with the requirement that neighboring vertices possess distinct colors. With real-world applications in scheduling, map coloring, and various optimization problems, graph coloring holds significance as a crucial area of study in both computer science and discrete mathematics. In 2015, Rosyida [5] introduced a new method for calculating the fuzzy chromatic set of a fuzzy graph using its δ -chromatic number. Additionally, the research delves into various characteristics of the fuzzy chromatic set in the context of fuzzy graphs. To enhance the thoroughness of the literature research and its findings, a Table 1 is presented outlining $\mathcal{FG}$ coloring.

Atanassov introduced the concept of intuitionistic fuzzy sets ($\mathcal{IFS}$) as a substantial enhancement to $\mathcal{FS}$ theory, incorporating the degree of hesitation associated with an element in [11]. In 2006, Parvathi and Karunambigai [14] introduced intuitionistic fuzzy graphs ($\mathcal{IFG}$). Additionally, to provide a comprehensive understanding of $\mathcal{IFS}$, Ejegwa *et al.* presented a concise summary of its key components, including definitions, operators, algebra, modal operators, and normalization in [13]. To further enrich the literature review, a structured overview of $\mathcal{IFG}$ is presented in the following Table 2.

In 1998, Smarandache [17] expanded the principles of $\mathcal{IFS}$ theory to encompass Neutrosophic Set ($\mathcal{NS}$) theory. In [18], Wang *et al.* introduced single-valued neutrosophic sets ($\mathcal{SVNS}$), utilizing the real standard interval [0,1], which is well-suited for practical situations. In 2016, Broumi *et al.* [19] developed the concept of neutrosophic graphs ($\mathcal{NG}$) by incorporating the idea of $\mathcal{SVNS}$ to create single-valued neutrosophic graphs ($\mathcal{SVNG}$). These $\mathcal{SVNG}$s serve as a generalization of $\mathcal{FG}$ and $\mathcal{IFG}$. They are especially valuable for addressing uncertain connections between nodes (vertices) in numerous problems. Neutrosophic graphs (NGs) extend classical and fuzzy graph models by incorporating truth-membership, indeterminacy-membership, and falsity-membership values for vertices and edges. In a classical graph, a vertex or edge either exists or does not exist, whereas a fuzzy graph assigns a membership degree to represent uncertainty. However, fuzzy graphs do not explicitly model indeterminate information. Neutrosophic graphs overcome this limitation by simultaneously representing the degree of truth, indeterminacy, and falsity associated with graph elements. Consequently, NGs provide a more powerful and flexible framework for analyzing systems characterized by uncertainty, incompleteness, inconsistency, and conflicting information. Table 3 offers an organized overview of $\mathcal{NG}$ to improve the depth of the research analysis and its results.

Recent developments in neutrosophic graph theory have significantly expanded its applicability to complex systems characterized by uncertainty, indeterminacy, and inconsistency. Kaviyarasu *et al.* [25] introduced connectivity indices for neutrosophic graphs and demonstrated their usefulness in modeling computer networks, highway systems, and transport network flows. Xiang [26] employed neutrosophic graph theory to evaluate organizational performance in higher education institutions, highlighting its effectiveness in handling uncertain relationships. Nagarajan *et al.* [27] proposed a Dynamic Neutrosophic Decision Matrix (DNDM) framework for smart city applications, illustrating the integration of neutrosophic concepts with urban decision-making processes. In the area of graph structure analysis, Sasipriya and Madireddy [28] investigated the distance spectrum and energy of single-valued neutrosophic graphs, providing important theoretical insights into graph properties. Furthermore, Muthuerulappan and Chelliah [29] studied edge-neighbor distinguishing proper coloring in neutrosophic graphs and explored its practical applications, thereby demonstrating the growing importance of coloring concepts in neutrosophic environments. In transportation and sustainability studies, Mary [30] utilized neutrosophic and plithogenic frameworks to analyze sustainable mobility problems through multi-criteria decision-making techniques.

Recent studies have demonstrated the growing applicability of neutrosophic graph theory in diverse scientific and engineering domains. Sm *et al.* [31] investigated neutrosophic topological indices, particularly the F-index and edge F-index, and applied these measures to optimize chemical reaction pathways under uncertain environments. Their work highlighted the effectiveness of neutrosophic graph structures in representing complex chemical systems and supporting optimization processes.

Syropoulos *et al.* [32] introduced the concept of neutrosophic graph rewriting as a computational model. Their study extended graph-rewriting techniques to neutrosophic environments, enabling the representation and processing of uncertain and indeterminate information in computational systems. The proposed framework provides a novel perspective for modeling dynamic systems through neutrosophic graph transformations.

Furthermore, Iftikhar *et al.* [33] proposed energy-based neutrosophic fuzzy graphs for cognition-driven organizational decision-making. Their approach incorporated graph-energy concepts into neutrosophic fuzzy environments to analyze organizational interactions and support decision-making under uncertainty. The results demonstrated the usefulness of neutrosophic graph models in addressing complex decision-support problems.

These contributions illustrate the increasing importance of neutrosophic graph theory in optimization, computational modeling, and decision-making. Motivated by these developments, the present work focuses on the study of neutrosophic chromatic numbers and their properties, providing a new graph-coloring framework for single-valued neutrosophic graphs and demonstrating its applicability through a traffic-light control system. Recently, several significant advancements have further expanded the scope of neutrosophic graph theory and its practical applications. Suriyakumar and Sudhakar [34] introduced the Randic index for neutrosophic graphs and demonstrated

Table 1: Literature review on $\mathcal{FG}$ coloring.

Author	Year	Results
Anjali Kishore & M.S. Sunitha [6]	2016	Application of $\mathcal{FG}$ using chromaticity
Rosyida *et al.* [7]	2019	New concept of $\mathcal{FG}$ Coloring
Isnaini Rosyida *et al.* [8]	2019	Application of Fuzzy Chromatic Number
Rupkumar Mahapatra *et al.* [9]	2020	Applications of Edge Colouring of $\mathcal{FG}$
Zengtai Gong & Jing Zhang [10]	2022	Application of $\mathcal{FG}$ Coloring

Table 2: Literature review on $\mathcal{IFG}$.

Author	Year	Results
R.Parvathi & M.G.Karunambigai [14]	2006	$\mathcal{IFG}$ and its properties
R.Parvathi *et al.* [15]	2009	Operations on $\mathcal{IFG}$
Muhammad Akram & Bijan Davvaz [16]	2012	Strong $\mathcal{IFG}$

Table 3: Literature review on $\mathcal{NG}$.

Author	Year	Results
Ridvan Sahin [20]	2019	$\mathcal{NG}$ with application
Sumera Naz *et al.* [21]	2017	Operations on $\mathcal{SVNG}$
Xiaohong Zhang [22]	2018	New inclusion relation of $\mathcal{NS}$ with applications
Avishek Chakraborty *et al.* [23]	2018	Different forms of neutrosophic numbers
Florentin Smarandache [24]	2020	Neutrosophic decision-making applications

its usefulness in analyzing structural characteristics and solving network-related problems under uncertainty. Their work extends classical topological indices to neutrosophic environments, providing new perspectives for graph-theoretic analysis. Jacob *et al.* [35] proposed directed neutrosophic graphs based on morphological operators to model directional relationships under uncertain conditions. Their methodology offers an effective framework for representing and processing complex structures in applications such as image analysis, pattern recognition, and network modeling. Fujita [36] presented quaternion fuzzy and quaternion neutrosophic graph models to represent reliability, ambiguity, and risk in information technology management systems. By incorporating quaternion-valued information, the proposed framework provides a richer representation of multidimensional uncertainty and broadens the applicability of neutrosophic graph theory in engineering and management sciences. Furthermore, Arokia and Radha [37] developed a shortest-path algorithm based on quadripartitioned single-valued neutrosophic refined numbers for uncertain network environments. Their approach improves decision-making in routing and network optimization by effectively handling multiple sources of uncertainty during path computation.

Although substantial progress has been made in the study of neutrosophic graphs and their applications, the concept of chromatic numbers based on α, β, γ-cuts, strong α, β, γ-cuts, and neutrosophic independent vertex sets remains largely unexplored. Existing studies primarily focus on connectivity measures, graph energy, decision-making frameworks, and coloring methodologies without developing a comprehensive neutrosophic chromatic number framework. Moreover, the behavior of neutrosophic chromatic numbers under graph operations, particularly the union of neutrosophic graphs, has received limited attention in the literature. Motivated by these research gaps, the present work introduces novel neutrosophic chromatic numbers, investigates their theoretical properties under union operations, and demonstrates their applicability through a traffic light management system.

1.1. Research gap

Although significant advancements have been made in neutrosophic graph theory, most existing studies focus on graph representations, connectivity measures, graph energy, decision-making models, and various applications under uncertain environments. Several researchers have investigated structural properties of neutrosophic graphs and their applications in transportation systems, computer networks, and smart-city frameworks. Furthermore, graph coloring concepts have been explored in neutrosophic settings; however, these studies primarily concentrate on coloring methodologies without establishing a comprehensive framework for neutrosophic chromatic numbers.

In particular, the determination of chromatic numbers based on α, β, γ-cuts and strong α, β, γ-cuts of neutrosophic graphs remains largely unexplored. Moreover, the relationship between neutrosophic chromatic numbers and neutrosophic independent vertex sets has not been adequately investigated in the literature. Existing studies also provide limited theoretical results concerning the behavior of chromatic numbers under graph operations, especially the union of neutrosophic graphs. In addition, practical applications of neutrosophic chromatic numbers to real-world traffic signal coordination and optimization problems are scarce.

To bridge these gaps, this paper introduces novel definitions of neutrosophic chromatic numbers based on α, β, γ-cuts, strong α, β, γ-cuts, and neutrosophic independent vertex sets. The study further establishes theoretical properties of these chromatic numbers under union operations and demonstrates their effectiveness through a traffic-light management application, thereby extending both the theoretical and practical scope of neutrosophic graph coloring.

1.2. Motivation of the paper

The development of the proposed chromatic-number framework for single-valued neutrosophic graphs (SVNGs) is motivated by the following observations and limitations of existing graph-coloring approaches:

1. Limitations of classical graph coloring
   Classical graph coloring assumes that the existence or absence of vertices and edges is completely known. Consequently, every adjacency relationship is treated as deterministic. However, many real-world systems involve uncertain, incomplete, and conflicting information, making classical graph-coloring models insufficient for accurately representing such environments.
2. Presence of uncertainty in real-world networks
   In practical applications such as transportation systems, communication networks, social networks, medical diagnosis, and decision-support systems, the relationships among entities are often uncertain and may vary over time. Therefore, a more flexible graph structure capable of incorporating uncertainty is required.
3. Need to handle indeterminate information
   Fuzzy graph models allow the representation of uncertainty through membership values, while intuitionistic fuzzy graphs consider both membership and non-membership information. Nevertheless, these frameworks do not explicitly represent indeterminate information. In many practical situations, available information may be incomplete, inconsistent, or partially unknown. Such circumstances necessitate a framework that can independently model indeterminacy.
4. Advantages of single-valued neutrosophic graphs
   single-valued neutrosophic graphs provide a more comprehensive representation of uncertainty through three independent membership functions, namely truth-membership, indeterminacy-membership, and falsity-membership. Consequently, SVNGs offer a richer mathematical environment for modeling complex systems than classical, fuzzy, or intuitionistic fuzzy graphs.
5. Lack of chromatic-number studies in SVNGs
   Although several investigations have been conducted on neutrosophic graphs, limited attention has been given to the development of chromatic-number concepts under a single-valued neutrosophic environment. Existing graph-coloring methods do not fully utilize the information provided by truth, indeterminacy, and falsity memberships simultaneously. This gap motivated the development of the proposed framework.
6. Need for cut-based coloring mechanisms
   Decision-makers often prefer to analyze graph structures under different confidence levels. The introduction of α-β-γ cuts enables the transformation of an SVNG into a crisp graph while preserving selected levels of truth, indeterminacy, and falsity information. This provides a flexible mechanism for studying graph-coloring behavior under different uncertainty thresholds.
7. Need for strong cut-based analysis
   In many applications, stricter conditions are required to identify highly reliable relationships. Therefore, strong α-β-γ cuts are introduced to provide a more restrictive representation of graph structures and to facilitate more robust coloring decisions under uncertainty.
8. Application to traffic signal control
   Traffic systems involve fluctuating traffic volumes, incomplete information, driver behavior variability, and uncertain conflict relationships among traffic movements. These characteristics make traffic-signal control a suitable application domain for SVNGs. The proposed chromatic framework provides a natural way to model conflicting traffic movements and determine compatible signal phases under uncertain conditions.
9. Generalization of existing coloring concepts
   The proposed chromatic numbers may be viewed as an extension of classical graph coloring to neutrosophic environments. When uncertainty and indeterminacy vanish, the proposed framework reduces to the corresponding crisp graph-coloring problem. Hence, the developed theory generalizes existing coloring concepts while retaining compatibility with traditional graph-theoretic principles.
10. Support for future decision-making applications
    The proposed framework is not limited to traffic management. It can potentially be applied to scheduling, resource allocation, communication networks, transportation planning, decision-support systems, and other optimization problems where uncertainty and indeterminacy play significant roles.

1.3. Strengths of the proposed framework

The proposed neutrosophic chromatic-number framework offers several important advantages:

1. It extends classical graph-coloring theory to single-valued neutrosophic graphs (SVNGs), enabling the representation of uncertainty, indeterminacy, and falsity.
2. It provides a more comprehensive modeling framework than classical, fuzzy, and intuitionistic fuzzy graph coloring by simultaneously considering truth-membership, indeterminacy-membership, and falsity-membership values.
3. The proposed α-β-γ cut and strong α-β-γ cut concepts allow flexible analysis of graph-coloring problems under different uncertainty thresholds.

4. The framework is mathematically rigorous and is supported by formal definitions, propositions, lemmas, and theorems.
5. It generalizes several existing graph-coloring concepts and reduces to classical graph-coloring models under suitable conditions.
6. The proposed methodology can accommodate uncertain and incomplete information frequently encountered in real-world systems.
7. The framework is applicable to practical problems such as traffic-light control, transportation networks, scheduling, resource allocation, communication systems, and decision-support applications.
8. The proposed model establishes a foundation for future research involving optimization algorithms, intelligent transportation systems, and advanced neutrosophic graph structures.

Advantages of neutrosophic graphs. Although fuzzy graphs and intuitionistic fuzzy graphs have been successfully applied to model uncertain systems, they possess certain limitations when dealing with incomplete and indeterminate information. A fuzzy graph represents only the degree of membership associated with vertices and edges, whereas an intuitionistic fuzzy graph incorporates both membership and non-membership degrees. However, neither framework explicitly models indeterminacy as an independent component. In contrast, single-valued neutrosophic graphs (SVNGs) simultaneously consider truth-membership, indeterminacy-membership, and falsity-membership values. This additional degree of freedom enables a more realistic representation of uncertainty, inconsistency, vagueness, and incomplete information. Consequently, SVNGs provide a more flexible and powerful framework for analyzing complex real-world systems than fuzzy and intuitionistic fuzzy graph models.

1.4. Significance of the proposed work

The significance of this work stems from its contribution to the development of graph-coloring theory in neutrosophic environments. By introducing neutrosophic chromatic numbers for single-valued neutrosophic graphs (SVNGs), the proposed framework extends traditional coloring concepts to situations involving uncertainty, indeterminacy, and inconsistency. Unlike classical, fuzzy, and intuitionistic fuzzy graph-coloring approaches, the proposed method simultaneously incorporates truth-membership, indeterminacy-membership, and falsity-membership information, thereby providing a more comprehensive representation of real-world systems.

The introduction of α-β-γ cuts and strong α-β-γ cuts offers a flexible mechanism for analyzing graph-coloring problems under different uncertainty levels. In addition to its theoretical contributions, the proposed framework demonstrates practical applicability through a traffic-light control problem, where uncertain traffic-flow conditions can be modeled more effectively. Therefore, this work establishes a foundation for future research in neutrosophic graph theory, optimization, decision-making, transportation systems, scheduling, and other applications involving uncertain network structures.

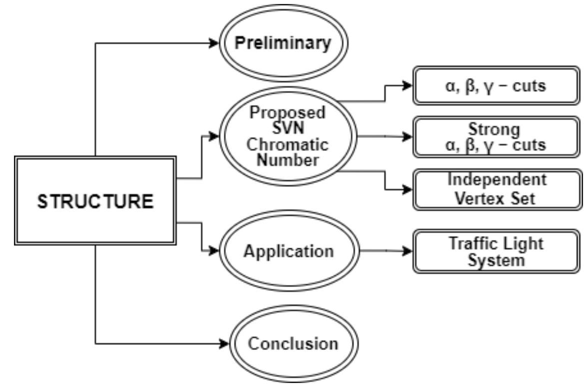

Figure 1: Outline of the paper.

1.5. Framework of the paper

The structure of the paper is as follows: Section 2 explores the key concepts pertaining to $\mathcal{NS}$ and $\mathcal{NG}$. Section 3 introduces various neutrosophic chromatic numbers and defines the union of $\mathcal{SVNG}$s, accompanied by a theorem. Section 4 presents an application of $\mathcal{NG}$ using these chromatic numbers, especially for the traffic-light problem. Section 5 discusses the results, limitations, and comparisons. In Section 6, overall conclusions are given. The concept was outlined in Figure 1, providing a clear understanding of the flow of our paper. To explore the uncharted territory of chromatic number in $\mathcal{NG}$. While previous research has extensively covered $\mathcal{NG}$ coloring, the specific investigation into their chromatic number has remained elusive. To bridge this gap, we've focused on $\mathcal{SVNG}$ coloring. Here are some key points highlighting the significance of our study:

- The objective of this study is to present a novel idea of $\mathcal{SVNG}$ coloring by utilizing fundamental sets (α,β,γ-cuts & strong α,β,γ-cuts) and independent sets.
- Also, we proposed the application of traffic light system problem in detail by calculating the chromatic number based on α,β,γ-cuts & strong - α,β,γ-cuts of $\mathcal{SVNG}$ and its operations. Moreover, a comparative analysis of the neutrosophic chromatic number is performed using the independent vertex set. At last, we are finding the optimality of traffic light problem to avoid maximum traffic incidents.

1.6. Main objectives of the present work

The main objectives of this work are as follows:

1. To introduce a novel chromatic-number framework for single-valued neutrosophic graphs (SVNGs) capable of handling uncertainty, indeterminacy, and inconsistency in graph-coloring problems.

2. To define and investigate new concepts of neutrosophic chromatic numbers, including chromatic numbers based on SVNGs, α-β-γ cuts, and strong α-β-γ cuts.
3. To establish the mathematical properties and theoretical foundations of the proposed chromatic-number framework through appropriate definitions, propositions, and theorems.
4. To extend classical graph-coloring theory to a neutrosophic environment by incorporating truth-membership, indeterminacy-membership, and falsity-membership information into the coloring process.
5. To provide a flexible mechanism for analyzing graph-coloring problems under different levels of uncertainty through cut-based and strong cut-based graph representations.
6. To demonstrate the applicability of the proposed framework through a traffic-light control problem, where traffic movements and conflict relationships are modeled using single-valued neutrosophic graphs.
7. To show how neutrosophic graph coloring can assist in grouping compatible traffic movements into signal phases under uncertain traffic conditions.
8. To establish a foundation for future research on optimization algorithms, decision-making models, transportation systems, and other real-world applications involving uncertain graph structures.

1.7. Relationship with other neutrosophic graph parameters

The proposed neutrosophic chromatic number is closely related to several graph-theoretic parameters in a neutrosophic environment. In particular, the neutrosophic clique number provides a lower bound for the neutrosophic chromatic number, whereas larger neutrosophic independent sets generally reduce the number of colors required. Furthermore, the neutrosophic chromatic number is directly influenced by the corresponding λ-cut and α-β-γ-cut graphs, whose structures depend on the truth-membership, indeterminacy-membership, and falsity-membership values assigned to vertices and edges. Consequently, the proposed chromatic framework is naturally connected with several important neutrosophic graph invariants. A detailed study of these relationships constitutes an interesting direction for future research.

1.8. Importance of the proposed work

A comparison of existing methods for determining the chromatic number is presented in the following Table 4.

2. Preliminaries

We will first revisit the fundamental definitions of $\mathcal{NS}$ and $\mathcal{NG}$ in this section. Also we recall some definition in $\mathcal{SVNS}$ and operations in $\mathcal{SVNG}$, which will play a crucial role in constructing chromatic numbers and their applications.

single-valued neutrosophic graphs. A single-valued neutrosophic graph (SVNG) is a generalization of a classical graph that incorporates uncertainty, indeterminacy, and falsity information into its structure. In an SVNG, each vertex and edge is associated with three independent membership degrees, namely truth-membership, indeterminacy-membership, and falsity-membership, whose values belong to the interval [0, 1]. Unlike classical and fuzzy graphs, SVNGs explicitly represent indeterminate information, allowing a more comprehensive description of complex systems characterized by incomplete, uncertain, or inconsistent data. Consequently, SVNGs provide a flexible mathematical framework for modeling and analyzing real-world networks under uncertainty.

Definition 2.1. [38] In a set X consisting of points (objects) and represented by s, a single-valued neutrosophic set ($\mathcal{SVNS}$) can be defined as a subset of X, where the function ϑ is determined by three functions known as truth-membership $\vartheta_t(s)$, indeterminacy-membership ϑ_i(s), and falsity-membership ϑ_f(s), such that ϑ_t(s), $\vartheta_i(s)$, $\vartheta_f(s) \in [0,1]$ and $0 \leq \vartheta_t(s) + \vartheta_i(s) + \vartheta_f(s) \leq 3$ for every s $\in$ X.

Two distinct methods exist for defining the inclusion relation of $\mathcal{NS}$ in the literature. The first, originally proposed by Smarandache [19–22], is termed the type-1 inclusion relation. The second, employed in certain papers [39, 40], is known as the type-2 inclusion relation. In this paper, we only work with type-1 inclusion relations for $\mathcal{NS}$ and NG.

Definition 2.2. [22] Consider two $\mathcal{SVNS}$, M and N, with membership functions ϑ_1 and ϑ_2 defined as M = {s, $\vartheta_{1(t)}(s), \vartheta_{1(i)}(s), \vartheta_{1(f)}(s)$: $\forall$ s $\in$ X } and N = {s, $\vartheta_{2(t)}(s), \vartheta_{2(i)}(s), \vartheta_{2(f)}(s) : \forall\ s \in X$ }. Then

1. $M \subseteq N \iff \vartheta_{1(t)}(s) \leq \vartheta_{2(t)}(s)$, $\vartheta_{1(i)}(s) \geq \vartheta_{2(i)}(s)$, $\vartheta_{1(f)}(s) \geq \vartheta_{2(f)}(s) \mid \forall\ s \in X$,
2. $M \cup N = \{$s,$(\vartheta_{1(t)}(s) \vee \vartheta_{2(t)}(s)), (\vartheta_{1(i)}(s) \wedge \vartheta_{2(i)}(s)), (\vartheta_{1(f)}(s) \wedge \vartheta_{2(f)}(s)) \mid \forall\ s \in X\}$,
3. $M \cap N = \{$s,$(\vartheta_{1(t)}(s) \wedge \vartheta_{2(t)}(s)), (\vartheta_{1(i)}(s) \vee \vartheta_{2(i)}(s)), (\vartheta_{1(f)}(s) \vee \vartheta_{2(f)}(s)) \mid \forall\ s \in X\}$,
4. $M^c = \{$ (s, $\vartheta_{1(f)}(s), 1 - \vartheta_{1(i)}(s), \vartheta_{1(t)}(s)) \mid \forall\ s \in X$ },
5. M = N $\iff M \subseteq N$ and $N \subseteq M \mid \forall\ s \in X$.

To simplify, we can denote an element in the $\mathcal{SVNS}$ as $\vartheta(s)$, where $\vartheta(s) = (\vartheta_t(s), \vartheta_i(s), \vartheta_f(s))$ and it is called a single-valued neutrosophic number ($\mathcal{SVNN}$).

Definition 2.3. [24] If M is a $\mathcal{SVNN}$ with ($\vartheta_t(s)$, $\vartheta_i(s)$, $\vartheta_f(s)$), then the single-valued neutrosophic score function ($\mathcal{SF}$) is defined as:

$$\begin{aligned}\mathcal{SF}(M) &= \frac{\vartheta_t(s) + (1 - \vartheta_i(s)) + (1 - \vartheta_f(s))}{3} \\ &= \frac{2 + \vartheta_t(s) - \vartheta_i(s) - \vartheta_f(s)}{3}.\end{aligned}$$

where $\mathcal{SF}$: M$\rightarrow$[0, 1]. For two $\mathcal{SVNN}$s, M_1 and M_2, if $\mathcal{SF}(M_1) > \mathcal{SF}(M_2)$ then $M_1 > M_2$.

Definition 2.4. [41] A crisp subset M over the set of real numbers $\mathbb{R}$ is considered a (α, β, γ)-cut set of a $\mathcal{SVNS}$, where :

Table 4: Comparison with the existing methods for finding chromatic number.

Domain	Year	Authors	fundamental sets	independent vertex set
$\mathcal{FG}$	2015	Isnaini Rosyida *et al.*	No	Yes
$\mathcal{FG}$	2019	Isnaini Rosyida *et al.*	No	Yes
$\mathcal{FG}$	2012	Arindam Dey & Anita Pal [43]	Yes (Using α-cuts)	No
$\mathcal{FG}$	2022	Zengtai Gong & Jing Zhang	Yes (Using α-cuts)	No
$\mathcal{IFG}$	2015	S.I. Mohideen & M.A. Rifayathali [44]	Yes (Using α,β-cuts)	No
$\mathcal{IFG}$	2018	M.A. Rifayathali *et al.* [45]	No	Yes
$\mathcal{SVNG}$	—	proposed work	Yes (Using α,β,γ-cuts and strong (α,β,γ)-cuts)	Yes

- $M(\alpha,\beta,\gamma) = \{s : \vartheta_t(s) \geq \alpha, \vartheta_i(s) \leq \beta, \vartheta_f(s) \leq \gamma\}$,
- $0 \leq \alpha \leq 1, 0 \leq \beta \leq 1, 0 \leq \gamma \leq 1$,
- $0 \leq \alpha+\beta+\gamma \leq 3$.

It should be noted that the proposed chromatic-number framework is developed for general single-valued neutrosophic graphs. The triangular single-valued neutrosophic numbers employed in the application section are used solely for representing and neutrosophicating traffic-flow data. The theoretical results presented in this study are independent of the specific neutrosophic-number representation and remain applicable to other forms of single-valued neutrosophic information, such as trapezoidal, interval-valued, pentagonal, and Gaussian neutrosophic numbers.

Definition 2.5. [23] A triangular single-valued neutrosophic number, denoted as S, is a number with the components $(l_1, l_2, l_3; m_1, m_2, m_3; n_1, n_2, n_3)$ and its truth-membership, indeterminacy-membership, and falsity-membership are delineated as follows:

$$\vartheta_t(s) = \begin{cases} \frac{\phi-l_1}{l_2-l_1} & \text{when } l_1 \leq \phi < l_2 \\ 1 & \text{when } \phi = l_2 \\ \frac{l_3-\phi}{l_3-l_2} & \text{when } l_2 < \phi \leq l_3 \\ 0 & \text{otherwise} \end{cases},$$

$$\vartheta_i(s) = \begin{cases} \frac{m_2-\phi}{m_2-m_1} & \text{when } m_1 \leq \phi < m_2 \\ 0 & \text{when } \phi = m_2 \\ \frac{\phi-m_2}{m_3-m_2} & \text{when } m_2 < \phi \leq m_3 \\ 1 & \text{otherwise} \end{cases},$$

$$\vartheta_f(s) = \begin{cases} \frac{n_2-\phi}{n_2-n_1} & \text{when } n_1 \leq \phi < n_2 \\ 0 & \text{when } \phi = n_2 \\ \frac{\phi-n_2}{n_3-n_2} & \text{when } n_2 < \phi \leq n_3 \\ 1 & \text{otherwise} \end{cases},$$

where $0 \leq \vartheta_t(s) + \vartheta_i(s) + \vartheta_f(s) \leq 3$.

Definition 2.6. [21] A set of vertices and edges, denoted by $\mathbb{G} = (\vartheta, \xi)$, form a single-valued neutrosophic graph $\mathcal{SVNG}$ with an underlying set $(\mathcal{V}^*, \mathcal{E}^*)$ where

1. The functions $\vartheta_t, \vartheta_i, \vartheta_f : \mathcal{V}^* \to [0,1]$ represent the degree of truth-membership, indeterminacy-membership, and falsity-membership of each element $s_i \in \mathcal{V}^*$. For all $s_i \in \mathcal{V}^*$, where $i = 1, 2, \ldots, n$, it must satisfy the condition $0 \leq \vartheta_t(s_i) + \vartheta_i(s_i) + \vartheta_f(s_i) \leq 3$.
2. The functions $\xi_t, \xi_i, \xi_f : \mathcal{E}^* \subseteq \mathcal{V}^* \times \mathcal{V}^* \to [0,1]$ represent the degree of truth-membership, indeterminacy-membership, and falsity-membership of the edge $(s_i, s_j) \in \mathcal{E}^*$, where $0 \leq \xi_t(s_i, s_j) + \xi_i(s_i, s_j) + \xi_f(s_i, s_j) \leq 3$ $\forall\ (s_i, s_j) \in \mathcal{E}^*$, and they also satisfy the following conditions:

$$\begin{aligned} &\xi_t(s_i, s_j) \leq \vartheta_t(s_i) \wedge \vartheta_t(s_j), \\ &\xi_i(s_i, s_j) \geq \vartheta_i(s_i) \vee \vartheta_i(s_j), \\ &\xi_f(s_i, s_j) \geq \vartheta_f(s_i) \vee \vartheta_f(s_j), \\ &\quad \forall (s_i, s_j) \in \mathcal{E}^*, \quad i, j = 1, 2, \ldots, n. \end{aligned}$$

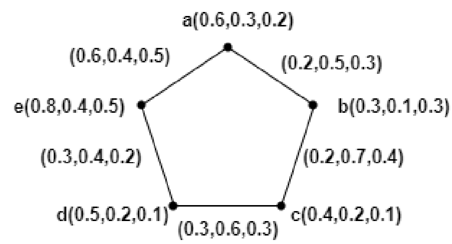

Figure 2: Example of a single-valued neutrosophic graph.

Figure 2 illustrates an instance of $\mathcal{SVNG}$ containing five vertices and five edges.

Definition 2.7. The mapping $\zeta : \mathcal{V}^*(\mathcal{G}^*) \to \mathbb{N}$ assigns a unique color to each vertex in the crisp graph $\mathcal{G}^* = (\mathcal{V}^*, \mathcal{E}^*)$, ensuring that adjacent vertices have different colors.

Definition 2.8. Let $\mathcal{G}^* = (\mathcal{V}^*, \mathcal{E}^*)$ be a crisp graph. A k-coloring function is a mapping $\zeta_k : \mathcal{V}^*(\mathcal{G}^*) \to \{1, 2, \ldots, k\}$ where $\zeta_k(m) \neq \zeta_k(n)$ if m and n are adjacent in $\mathcal{G}^*$. The chromatic number $(\mathcal{CN})$ of a graph $\mathcal{G}^*$ is the minimum value of k in $\mathcal{G}^*$and is represented as $\chi(\mathcal{G}^*)$.

Definition 2.9. [10] A subset S of the vertex set $\mathcal{V}^*$, known as a clique, is defined within a set of crisp graphs $\mathcal{G}^*$. This subset forms a complete graph when induced as a subgraph.

Definition 2.10. [21], [42] Let two $\mathcal{SVNG}$s be considered, namely $\mathbb{G}_1 = (\vartheta_1, \xi_1)$ and $\mathbb{G}_2 = (\vartheta_2, \xi_2)$. Let $\mathcal{G}_1^* = (\mathcal{V}_1^*, \mathcal{E}_1^*)$ and $\mathcal{G}_2^* = (\mathcal{V}_2^*, \mathcal{E}_2^*)$ be the underlying graphs corresponding to

$\mathbb{G}_1$ and $\mathbb{G}_2$ respectively. The union of $\mathbb{G}_1$ and $\mathbb{G}_2$, denoted as $\mathbb{G}_1 \cup \mathbb{G}_2 = (\vartheta_1 \cup \vartheta_2, \xi_1 \cup \xi_2)$, is delineated in the way that follows:

$$(\vartheta_{1(t)} \cup \vartheta_{2(t)})(s) = \begin{cases} \vartheta_{1(t)}(s) & \text{if } s \in \mathcal{V}_1^* \setminus \mathcal{V}_2^*, \\ \vartheta_{2(t)}(s) & \text{if } s \in \mathcal{V}_2^* \setminus \mathcal{V}_1^*, \\ \max\{\vartheta_{1(t)}(s), \vartheta_{2(t)}(s)\} & \text{if } s \in \mathcal{V}_1^* \cap \mathcal{V}_2^*. \end{cases}$$

$$(\vartheta_{1(i)} \cup \vartheta_{2(i)})(s) = \begin{cases} \vartheta_{1(i)}(s) & \text{if } s \in \mathcal{V}_1^* \setminus \mathcal{V}_2^*, \\ \vartheta_{2(i)}(s) & \text{if } s \in \mathcal{V}_2^* \setminus \mathcal{V}_1^*, \\ \min\{\vartheta_{1(i)}(s), \vartheta_{2(i)}(s)\} & \text{if } s \in \mathcal{V}_1^* \cap \mathcal{V}_2^*. \end{cases}$$

$$(\vartheta_{1(f)} \cup \vartheta_{2(f)})(s) = \begin{cases} \vartheta_{1(f)}(s) & \text{if } s \in \mathcal{V}_1^* \setminus \mathcal{V}_2^*, \\ \vartheta_{2(f)}(s) & \text{if } s \in \mathcal{V}_2^* \setminus \mathcal{V}_1^*, \\ \min\{\vartheta_{1(f)}(s), \vartheta_{2(f)}(s)\} & \text{if } s \in \mathcal{V}_1^* \cap \mathcal{V}_2^*. \end{cases}$$

$(\xi_{1(t)} \cup \xi_{2(t)})(s_1 s_2) =$

$$\begin{cases} \xi_{1(t)}(s_1 s_2) & \text{if } s_1 s_2 \in \mathcal{E}_1^* \setminus \mathcal{E}_2^*, \\ \xi_{2(t)}(s_1 s_2) & \text{if } s_1 s_2 \in \mathcal{E}_2^* \setminus \mathcal{E}_1^*, \\ \max\{\xi_{1(t)}(s_1 s_2), \xi_{2(t)}(s_1 s_2)\} & \text{if } s_1 s_2 \in \mathcal{E}_1^* \cap \mathcal{E}_2^*. \end{cases}$$

$(\xi_{1(i)} \cup \xi_{2(i)})(s_1 s_2) =$

$$\begin{cases} \xi_{1(i)}(s_1 s_2) & \text{if } s_1 s_2 \in \mathcal{E}_1^* \setminus \mathcal{E}_2^*, \\ \xi_{2(i)}(s_1 s_2) & \text{if } s_1 s_2 \in \mathcal{E}_2^* \setminus \mathcal{E}_1^*, \\ \min\{\xi_{1(i)}(s_1 s_2), \xi_{2(i)}(s_1 s_2)\} & \text{if } s_1 s_2 \in \mathcal{E}_1^* \cap \mathcal{E}_2^*. \end{cases}$$

$(\xi_{1(f)} \cup \xi_{2(f)})(s_1 s_2) =$

$$\begin{cases} \xi_{1(f)}(s_1 s_2) & \text{if } s_1 s_2 \in \mathcal{E}_1^* \setminus \mathcal{E}_2^*, \\ \xi_{2(f)}(s_1 s_2) & \text{if } s_1 s_2 \in \mathcal{E}_2^* \setminus \mathcal{E}_1^*, \\ \min\{\xi_{1(f)}(s_1 s_2), \xi_{2(f)}(s_1 s_2)\} & \text{if } s_1 s_2 \in \mathcal{E}_1^* \cap \mathcal{E}_2^*. \end{cases}$$

Definition 2.11. [38] Consider two $\mathcal{SVNG}$s as $\mathbb{G}_1 = (\vartheta_1, \xi_1)$ and $\mathbb{G}_2 = (\vartheta_2, \xi_2)$. Let $\mathcal{G}_1^* = (\mathcal{V}_1^*, \mathcal{E}_1^*)$ and $\mathcal{G}_2^* = (\mathcal{V}_2^*, \mathcal{E}_2^*)$ be the corresponding underlying graphs, then the intersection of $\mathbb{G}_1$ and $\mathbb{G}_2$ represented as $\mathbb{G}_1 \cap \mathbb{G}_2 = (\vartheta_1 \cap \vartheta_2, \xi_1 \cap \xi_2)$, is defined as follows:

$$(\vartheta_{1(t)} \cap \vartheta_{2(t)})(s) = \begin{cases} \vartheta_{1(t)}(s) & \text{if } s \in \mathcal{V}_1^* \setminus \mathcal{V}_2^*, \\ \vartheta_{2(t)}(s) & \text{if } s \in \mathcal{V}_2^* \setminus \mathcal{V}_1^*, \\ \min\{\vartheta_{1(t)}(s), \vartheta_{2(t)}(s)\} & \text{if } s \in \mathcal{V}_1^* \cap \mathcal{V}_2^*. \end{cases}$$

$$(\vartheta_{1(i)} \cap \vartheta_{2(i)})(s) = \begin{cases} \vartheta_{1(i)}(s) & \text{if } s \in \mathcal{V}_1^* \setminus \mathcal{V}_2^*, \\ \vartheta_{2(i)}(s) & \text{if } s \in \mathcal{V}_2^* \setminus \mathcal{V}_1^*, \\ \max\{\vartheta_{1(i)}(s), \vartheta_{2(i)}(s)\} & \text{if } s \in \mathcal{V}_1^* \cap \mathcal{V}_2^*. \end{cases}$$

$$(\vartheta_{1(f)} \cap \vartheta_{2(f)})(s) = \begin{cases} \vartheta_{1(f)}(s) & \text{if } s \in \mathcal{V}_1^* \setminus \mathcal{V}_2^*, \\ \vartheta_{2(f)}(s) & \text{if } s \in \mathcal{V}_2^* \setminus \mathcal{V}_1^*, \\ \max\{\vartheta_{1(f)}(s), \vartheta_{2(f)}(s)\} & \text{if } s \in \mathcal{V}_1^* \cap \mathcal{V}_2^*. \end{cases}$$

$(\xi_{1(t)} \cap \xi_{2(t)})(s_1 s_2) =$

$$\begin{cases} \xi_{1(t)}(s_1 s_2) & \text{if } s_1 s_2 \in \mathcal{E}_1^* \setminus \mathcal{E}_2^*, \\ \xi_{2(t)}(s_1 s_2) & \text{if } s_1 s_2 \in \mathcal{E}_2^* \setminus \mathcal{E}_1^*, \\ \min\{\xi_{1(t)}(s_1 s_2), \xi_{2(t)}(s_1 s_2)\} & \text{if } s_1 s_2 \in \mathcal{E}_1^* \cap \mathcal{E}_2^*. \end{cases}$$

$(\xi_{1(i)} \cap \xi_{2(i)})(s_1 s_2) =$

$$\begin{cases} \xi_{1(i)}(s_1 s_2) & \text{if } s_1 s_2 \in \mathcal{E}_1^* \setminus \mathcal{E}_2^*, \\ \xi_{2(i)}(s_1 s_2) & \text{if } s_1 s_2 \in \mathcal{E}_2^* \setminus \mathcal{E}_1^*, \\ \max\{\xi_{1(i)}(s_1 s_2), \xi_{2(i)}(s_1 s_2)\} & \text{if } s_1 s_2 \in \mathcal{E}_1^* \cap \mathcal{E}_2^*. \end{cases}$$

$(\xi_{1(f)} \cap \xi_{2(f)})(s_1 s_2) =$

$$\begin{cases} \xi_{1(f)}(s_1 s_2) & \text{if } s_1 s_2 \in \mathcal{E}_1^* \setminus \mathcal{E}_2^*, \\ \xi_{2(f)}(s_1 s_2) & \text{if } s_1 s_2 \in \mathcal{E}_2^* \setminus \mathcal{E}_1^*, \\ \max\{\xi_{1(f)}(s_1 s_2), \xi_{2(f)}(s_1 s_2)\} & \text{if } s_1 s_2 \in \mathcal{E}_1^* \cap \mathcal{E}_2^*. \end{cases}$$

3. Neutrosophic chromatic number

In this section we expand the union of two $\mathcal{SVNG}$s to the union of three $\mathcal{SVNG}$s and introduce a neutrosophic chromatic number based on α,β,γ - cuts as well as strong α,β,γ - cuts of the $\mathcal{SVNG}$ using fundamental set. Additionally, we put forth a proposal for the neutrosophic chromatic number of $\mathcal{SVNG}$s, using independent vertex set, along with illustrative examples.

Motivation of the α-β-γ-Cut Chromatic Number. In a single-valued neutrosophic graph (SVNG), vertices and edges are characterized by truth-membership, indeterminacy-membership, and falsity-membership values. Since graph coloring is traditionally defined for crisp graphs, it is necessary to transform the SVNG into a crisp graph before determining its chromatic number. This transformation is achieved through the use of α-β-γ cuts.

For prescribed threshold values α, β, and γ, only those vertices and edges satisfying the required truth, indeterminacy, and falsity conditions are retained in the resulting crisp graph. The chromatic number of this derived graph is called the α-β-γ-cut neutrosophic chromatic number. Consequently, the coloring process can be analyzed under different uncertainty levels by varying the threshold parameters.

Definition 3.1. Let $\tilde{\mathbb{G}} = (\vartheta, \tilde{\xi})$ be the $\mathcal{SVNG}$ of the graph $\mathcal{G}^* = (\mathcal{V}^*, \mathcal{E}^*)$, where ϑ is a set of crisp vertices and $\tilde{\xi} = (\tilde{\xi}_t, \tilde{\xi}_i, \tilde{\xi}_f)$ is a single-valued neutrosophic relation on $\mathcal{E}^*$ such that $\tilde{\xi}_t(s_i s_j) \leq \vartheta_t(s_i) \wedge \vartheta_t(s_j), \tilde{\xi}_i(s_i s_j) \geq \vartheta_i(s_i) \vee \vartheta_i(s_j), \tilde{\xi}_f(s_i s_j) \geq \vartheta_f(s_i) \vee \vartheta_f(s_j)$ and $0 \leq \tilde{\xi}_t(s_i s_j) + \tilde{\xi}_i(s_i s_j) + \tilde{\xi}_f(s_i s_j) \leq 3 \ \forall \ s_i, s_j \in \vartheta$.

Definition 3.2. Consider three $\mathcal{SVNG}$s, $\tilde{\mathbb{G}}_1 = (\vartheta_1, \tilde{\xi}_1)$, $\tilde{\mathbb{G}}_2 = (\vartheta_2, \tilde{\xi}_2)$, and $\tilde{\mathbb{G}}_3 = (\vartheta_3, \tilde{\xi}_3)$, each with crisp vertices and neutrosophic edges of $\mathcal{G}_1^* = (\mathcal{V}_1^*, \mathcal{E}_1^*)$, $\mathcal{G}_2^* = (\mathcal{V}_2^*, \mathcal{E}_2^*)$ and $\mathcal{G}_3^* = (\mathcal{V}_3^*, \mathcal{E}_3^*)$ respectively. The union $\tilde{\mathbb{G}}_1 \cup \tilde{\mathbb{G}}_2 \cup \tilde{\mathbb{G}}_3$ of SVNGs $\tilde{\mathbb{G}}_1$, $\tilde{\mathbb{G}}_2$, and $\tilde{\mathbb{G}}_3$, is defined as follows,

$$\tilde{\xi}_1 \cup \tilde{\xi}_2 \cup \tilde{\xi}_3(mn) = \begin{cases} (\tilde{\xi}_{1(t)}(mn), \tilde{\xi}_{1(i)}(mn), \tilde{\xi}_{1(f)}(mn)), \\ \quad \text{if } mn \in \mathcal{E}_1^*,\ mn \notin \mathcal{E}_2^*, \mathcal{E}_3^*; \\ (\tilde{\xi}_{2(t)}(mn), \tilde{\xi}_{2(i)}(mn), \tilde{\xi}_{2(f)}(mn)), \\ \quad \text{if } mn \in \mathcal{E}_2^*,\ mn \notin \mathcal{E}_1^*, \mathcal{E}_3^*; \\ (\tilde{\xi}_{3(t)}(mn), \tilde{\xi}_{3(i)}(mn), \tilde{\xi}_{3(f)}(mn)), \\ \quad \text{if } mn \in \mathcal{E}_3^*,\ mn \notin \mathcal{E}_1^*, \mathcal{E}_2^*; \\ \begin{pmatrix} \max(\tilde{\xi}_{1(t)}(mn), \tilde{\xi}_{2(t)}(mn)), \\ \min(\tilde{\xi}_{1(i)}(mn), \tilde{\xi}_{2(i)}(mn)), \\ \min(\tilde{\xi}_{1(f)}(mn), \tilde{\xi}_{2(f)}(mn)) \end{pmatrix}, \\ \quad \text{if } mn \in \mathcal{E}_1^* \cap \mathcal{E}_2^*; \\ \begin{pmatrix} \max(\tilde{\xi}_{2(t)}(mn), \tilde{\xi}_{3(t)}(mn)), \\ \min(\tilde{\xi}_{2(i)}(mn), \tilde{\xi}_{3(i)}(mn)), \\ \min(\tilde{\xi}_{2(f)}(mn), \tilde{\xi}_{3(f)}(mn)) \end{pmatrix}, \\ \quad \text{if } mn \in \mathcal{E}_2^* \cap \mathcal{E}_3^*; \\ \begin{pmatrix} \max(\tilde{\xi}_{3(t)}(mn), \tilde{\xi}_{1(t)}(mn)), \\ \min(\tilde{\xi}_{3(i)}(mn), \tilde{\xi}_{1(i)}(mn)), \\ \min(\tilde{\xi}_{3(f)}(mn), \tilde{\xi}_{1(f)}(mn)) \end{pmatrix}, \\ \quad \text{if } mn \in \mathcal{E}_3^* \cap \mathcal{E}_1^*; \\ \begin{pmatrix} \max(\tilde{\xi}_{1(t)}(mn), \tilde{\xi}_{2(t)}(mn), \tilde{\xi}_{3(t)}(mn)), \\ \min(\tilde{\xi}_{1(i)}(mn), \tilde{\xi}_{2(i)}(mn), \tilde{\xi}_{3(i)}(mn)), \\ \min(\tilde{\xi}_{1(f)}(mn), \tilde{\xi}_{2(f)}(mn), \tilde{\xi}_{3(f)}(mn)) \end{pmatrix}, \\ \quad \text{if } mn \in \mathcal{E}_1^* \cap \mathcal{E}_2^* \cap \mathcal{E}_3^*. \end{cases}$$

3.1. Chromatic number ($\mathcal{CN}$) using neutrosophic fundamental set

Definition 3.3. Let

$$S = (\alpha_1, \beta_1, \gamma_1), (\alpha_2, \beta_2, \gamma_2), \ldots, (\alpha_k, \beta_k, \gamma_k)$$

be the fundamental set of $\tilde{\mathbb{G}}$, where the elements are ordered such that

$$\alpha_1 \leq \alpha_2 \leq \cdots \leq \alpha_k,$$

$$\beta_1 \geq \beta_2 \geq \cdots \geq \beta_k,$$

and

$$\gamma_1 \geq \gamma_2 \geq \cdots \geq \gamma_k.$$

The increasing sequence of α values represents progressively stricter truth-membership requirements, whereas the decreasing sequences of β and γ represent progressively stricter indeterminacy and falsity constraints, respectively. For each $(\alpha_i, \beta_i, \gamma_i) \in S$, the corresponding crisp graph $G_{\alpha_i,\beta_i,\gamma_i}(V, E_{\alpha_i,\beta_i,\gamma_i})$ is obtained through the (α, β, γ)-cut or strong (α, β, γ)-cut defined below. The ordering of the parameters is chosen to reflect progressively stricter cut conditions in the neutrosophic environment. Since a vertex or edge is included in the (α, β, γ)-cut graph only when its truth-membership value is at least α, increasing the value of α imposes a more restrictive inclusion criterion. Therefore, the sequence $\alpha_1 \leq \alpha_2 \leq \cdots \leq \alpha_k$ represents increasingly stringent truth-membership requirements. On the other hand, indeterminacy-membership and falsity-membership values must not exceed the prescribed thresholds β and γ, respectively. Consequently, decreasing these thresholds imposes stricter constraints on uncertainty and falsity. For this reason, the sequences $\beta_1 \geq \beta_2 \geq \cdots \geq \beta_k$ and $\gamma_1 \geq \gamma_2 \geq \cdots \geq \gamma_k$ are arranged in non-increasing order. This ordering generates a nested family of cut graphs that enables the systematic study of graph-coloring behavior under different levels of truth, indeterminacy, and falsity.

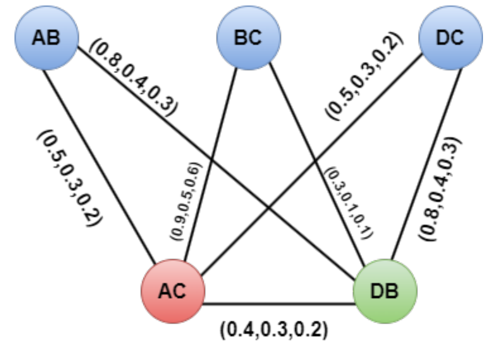

Figure 3: Single-valued neutrosophic graph.

Definition 3.4. The notation used to represent the $\mathcal{CN}$ of the crisp graph $G_{\alpha_i,\beta_i,\gamma_i}$ is $\chi(G_{\alpha_i,\beta_i,\gamma_i})$. Similarly, the $\mathcal{CN}$ of the $\mathcal{SVNG}$ $\tilde{\mathbb{G}}$ is denoted as $\chi(\tilde{\mathbb{G}})$ and can be determined as

$$\chi(\tilde{\mathbb{G}}) = \max\{\chi(G_{\alpha_i,\beta_i,\gamma_i}) \mid \alpha_i, \beta_i, \gamma_i \in S\}.$$

3.2. Chromatic number ($\mathcal{CN}$) using neutrosophic independent vertex set

Definition 3.5. Let $\tilde{\mathbb{G}}(\vartheta, \tilde{\xi})$ be a $\mathcal{SVNG}$. Given $\lambda \in [0, 1]$, where $\lambda_t, \lambda_i, \lambda_f : \lambda \to [0, 1]$, let $S \subseteq \vartheta$ be an independent set defined by

$$\tilde{\xi}_t(mn) \leq \lambda_t, \qquad \tilde{\xi}_i(mn) \geq \lambda_i,$$
$$\tilde{\xi}_f(mn) \geq \lambda_f \qquad \forall\, m, n \in S..$$

This is also known as λ-neutrosophic independent set and it is represented by S^λ.

Example 3.1. From Figure 3, we can say that the vertices AC and DB are λ-neutrosophic independent for $\lambda = (0.4, 0.3, 0.2)$. In case of vertices like AB and BC are λ-neutrosophic independent on $\lambda = (0, 1, 1)$.

Definition 3.6. Given $\lambda_t, \lambda_i, \lambda_f \in [0, 1]$, a k-coloring of a $\mathcal{SVNG}$ $\tilde{\mathbb{G}}(\vartheta, \tilde{\xi})$ is delineated as a function $F : \vartheta \to \{1, 2, \ldots, k\}$ that satisfies the condition: $F(m) = F(n)$ if $\tilde{\xi}_t(mn) \leq \lambda_t$, $\tilde{\xi}_i(mn) \geq \lambda_i$ and $\tilde{\xi}_f(mn) \geq \lambda_f$. The minimum value of k required for the k-coloring of $\tilde{\mathbb{G}}$ is known as the λ-$\mathcal{CN}$ of $\tilde{\mathbb{G}}$ and is denoted as $\chi^\lambda(\tilde{\mathbb{G}})$.

Definition 3.7. The neutrosophic $\mathcal{CN}$ of a given $\mathcal{SVNG}$ $\tilde{\mathbb{G}}(\vartheta, \tilde{\xi})$ with n elements, is represented as $\tilde{\chi}(\tilde{\mathbb{G}})$, is a SVNS defined as $\tilde{\chi}(\tilde{\mathbb{G}}) = \{(k, \mathcal{L}_{\tilde{\chi}}(k)) \mid k = 1, \ldots, n\}$, where $\mathcal{L}_{\tilde{\chi}}(k) = \max\{1-\lambda_t, 1-\lambda_i, 1-\lambda_f \mid \lambda_t, \lambda_i, \lambda_f \in [0,1]$ and $\chi^{\lambda}(\tilde{\mathbb{G}}) = k\}$, representing the degree of membership of the number k in the neutrosophic $\mathcal{CN}$ $\tilde{\chi}$.

Remark 3.1. The λ-$\mathcal{CN}$ $\chi^{(0,1,1)}(\tilde{\mathbb{G}})$, denoted as k_0, where $\mathcal{L}_{\tilde{\chi}}(k_0) = (1,0,0)$ in the neutrosophic chromatic set $\tilde{\chi}(\tilde{\mathbb{G}})$, equals the $\mathcal{CN}$ $\chi(\mathcal{G}^*)$ of the crisp graph $\mathcal{G}^*$.

Remark 3.2. In a $\mathcal{SVNG}$ $\tilde{\mathbb{G}}(\vartheta, \tilde{\xi})$ with n vertices, where $\vartheta = \{s_1, \ldots, s_n\}$, the only partition that results in $\chi^{\lambda}(\tilde{\mathbb{G}}) = n \ \forall \ \lambda \in [0,1]$ is the set $\{S_1^{\lambda}, \ldots, S_n^{\lambda}\}$, where $S_i^{\lambda} = \{s_i\} \ \forall \ i = 1, \ldots, n$. Therefore, $\mathcal{L}_{\tilde{\chi}}(n) = \vee\{1-\lambda \,|\, \chi^{\lambda}(\tilde{\mathbb{G}}) = n\} = 1$.

Example 3.2. Let us take a $\mathcal{SVNG}$ $\tilde{\mathbb{G}}(\vartheta, \tilde{\xi})$, where ϑ is a vertex set consisting of five vertices and the neutrosophic edge set $\tilde{\xi}$ consists of seven edges, as shown in Figure 3.

$$\vartheta = \{AB,\ BC,\ DC,\ AC,\ DB\},$$

$$\tilde{\xi} = \{(0.3, 0.1, 0.1),\ (0.4, 0.3, 0.2),\ (0.5, 0.3, 0.2),\ (0.8, 0.4, 0.3),\ (0.9, 0.5, 0.6)\}.$$

Based on Definition-3.7 and the partitions of ϑ and λ-$\mathcal{CN}$s presented in Table-5, we determine the neutrosophic $\mathcal{CN}$ of $\tilde{\mathbb{G}}$.

$$\tilde{\chi}(\tilde{\mathbb{G}}) = \{(3, (1,0,0)), (2, (0.2, 0.7, 0.4)), (1, (0.6, 0.5, 0.1))\}.$$

As λ increases, there is a tendency for the λ-$\mathcal{CN}$ to decrease. This is also observed in the neutrosophic $\mathcal{CN}$ $\tilde{\chi}$, where higher values of λ lead to a decrease in the degrees of $\mathcal{L}_{\tilde{\chi}}(k)$.

Lemma 3.1. For a $\mathcal{SVNG}$ $\tilde{\mathbb{G}}(\vartheta, \tilde{\xi})$ with $|\vartheta|$=n, let $\mathcal{G}^*(\mathcal{V}^*, \mathcal{E}^*)$ denote the crisp underlying graph of $\tilde{\mathbb{G}}$. If S denotes the λ-$\mathcal{CN}$s of $\tilde{\mathbb{G}}$ $\forall$ $\lambda \in$ [0,1], then the neutrosophic chromatic set $\tilde{\chi}(\tilde{\mathbb{G}})$ has $\mathcal{L}_{\tilde{\chi}}(s) = \mathcal{L}_{\tilde{\chi}}(p) = 1$ for any s,p $\in$ S such that $k_0 \le s \le p < n$.

Proof. Based on Remarks 3.1 and 3.2, it can be concluded that $\mathcal{L}_{\tilde{\chi}}(k_0) = 1$ and $\mathcal{L}_{\tilde{\chi}}(n) = 1$. Since, $k_0 \le s \le p < n$, it can be determined that $1 \le \mathcal{L}_{\tilde{\chi}}(s) \le \mathcal{L}_{\tilde{\chi}}(p) = 1$. Therefore, it can be stated that $\mathcal{L}_{\tilde{\chi}}(s) = \mathcal{L}_{\tilde{\chi}}(p) = 1$. □

In other words, above lemma-3.1 states that If $\chi^{\lambda}(\tilde{\mathbb{G}}) = i$ has the degree $\mathcal{L}_{\tilde{\chi}}(i) = 1$ and i $\neq$ n then $\mathcal{L}_{\tilde{\chi}}(i) = 1 \ \forall \ i \le k < n$.

Theorem 3.1. Let us consider $\tilde{\mathbb{G}}_1(\vartheta_1, \tilde{\xi}_1)$, $\tilde{\mathbb{G}}_2(\vartheta_2, \tilde{\xi}_2)$ and $\tilde{\mathbb{G}}_3(\vartheta_3, \tilde{\xi}_3)$ be three $\mathcal{SVNG}$s with $|\vartheta_1| = m_1$, $|\vartheta_2| = m_2$ and $|\vartheta_3| = m_3$. Consider $\tilde{\chi}(\tilde{\mathbb{G}}_1)$, $\tilde{\chi}(\tilde{\mathbb{G}}_2)$ and $\tilde{\chi}(\tilde{\mathbb{G}}_3)$ be neutrosophic $\mathcal{CN}s$ of $\tilde{\mathbb{G}}_1$, $\tilde{\mathbb{G}}_2$ and $\tilde{\mathbb{G}}_3$. Assume that ϑ_1, ϑ_2, and ϑ_3 are pairwise disjoint. If $\tilde{\mathbb{G}} = \tilde{\mathbb{G}}_1 \cup \tilde{\mathbb{G}}_2 \cup \tilde{\mathbb{G}}_3$ then $\tilde{\chi}(\tilde{\mathbb{G}}) = \{(k, \mathcal{L}_{\tilde{\chi}}(k))\}$ where

$$\mathcal{L}_{\tilde{\chi}}(k) = \begin{cases} \min\{\mathcal{L}_{\tilde{\chi}_1}(k), \mathcal{L}_{\tilde{\chi}_2}(k), \mathcal{L}_{\tilde{\chi}_3}(k)\} & \text{if } 1 \le k \le \min\{m_1, m_2, m_3\}, \\ \mathcal{L}_{\tilde{\chi}_1}(k) & \text{if } \min\{m_1,m_2,m_3\} < k \le m_1, \text{ where } m_1 = \max\{m_1,m_2,m_3\}, \\ \mathcal{L}_{\tilde{\chi}_2}(k) & \text{if } \min\{m_1,m_2,m_3\} < k \le m_2, \text{ where } m_2 = \max\{m_1,m_2,m_3\}, \\ \mathcal{L}_{\tilde{\chi}_3}(k) & \text{if } \min\{m_1,m_2,m_3\} < k \le m_3, \text{ where } m_3 = \max\{m_1,m_2,m_3\}, \\ (1,0,0) & \text{if } \max\{m_1,m_2,m_3\} < k \le m_1+m_2+m_3 \end{cases}.$$

Proof. Let $\vartheta_1 = \{u_1, u_2, \ldots, u_{m_1}\}$, $\vartheta_2 = \{v_1, v_2, \ldots, v_{m_2}\}$ and $\vartheta_3 = \{w_1, w_2, \ldots, w_{m_3}\}$. Let $\tilde{\chi}(\tilde{\mathbb{G}}_1) = \{(k, \mathcal{L}_{\tilde{\chi}_1}(k) \mid k = 1, \ldots, m_1\}$, $\tilde{\chi}(\tilde{\mathbb{G}}_2) = \{(k, \mathcal{L}_{\tilde{\chi}_2}(k) \mid k = 1, \ldots, m_2\}$ and $\tilde{\chi}(\tilde{\mathbb{G}}_3) = \{(k, \mathcal{L}_{\tilde{\chi}_3}(k) \mid k = 1, \ldots, m_3\}$ be neutrosophic $\mathcal{CN}s$ of $\tilde{\mathbb{G}}_1$, $\tilde{\mathbb{G}}_2$ and $\tilde{\mathbb{G}}_3$ respectively. There are three cases that we are taking into consideration:

For $1 \le k \le \min\{m_1, m_2, m_3\}$

According to Definition-3.7, for every value of k, there exist a $\lambda_{k_1} \in [0,1]$ which allows us to construct a partition $\{P_1^{\lambda_{k_1}}, P_2^{\lambda_{k_1}}, \ldots, P_k^{\lambda_{k_1}}\}$ on ϑ_1 which gives

$$\chi^{\lambda_{k_1}}(\tilde{\mathbb{G}}_1) = k \quad \text{and}$$
$$\mathcal{L}_{\tilde{\chi}_1}(k) = \{1-\lambda_{t_{(k_1)}}, 1-\lambda_{i_{(k_1)}}, 1-\lambda_{f_{(k_1)}}\}.$$

Similarly, $\exists$ $\lambda_{k_2} \in [0,1]$ such that we can construct a partition $\{Q_1^{\lambda_{k_2}}, Q_2^{\lambda_{k_2}}, \ldots, Q_k^{\lambda_{k_2}}\}$ on ϑ_2 that yields,

$$\chi^{\lambda_{k_2}}(\tilde{\mathbb{G}}_2) = k \quad \text{and}$$
$$\mathcal{L}_{\tilde{\chi}_2}(k) = \{1-\lambda_{t_{(k_2)}}, 1-\lambda_{i_{(k_2)}}, 1-\lambda_{f_{(k_2)}}\}.$$

Also, $\exists$ $\lambda_{k_3} \in [0,1]$ such that we can construct a partition $\{R_1^{\lambda_{k_3}}, R_2^{\lambda_{k_3}}, \ldots, R_k^{\lambda_{k_3}}\}$ on ϑ_3 which gives

$$\chi^{\lambda_{k_3}}(\tilde{\mathbb{G}}_3) = k \quad \text{and}$$
$$\mathcal{L}_{\tilde{\chi}_3}(k) = \{1-\lambda_{t_{(k_3)}}, 1-\lambda_{i_{(k_3)}}, 1-\lambda_{f_{(k_3)}}\}.$$

Further, we choose $\lambda = \max\{\lambda_{k_1}, \lambda_{k_2}, \lambda_{k_3}\}$ and a partition formed

$$\begin{aligned} S = \{S_1^{\lambda} &= P_1^{\lambda_{k_1}} \cup Q_1^{\lambda_{k_2}} \cup R_1^{\lambda_{k_3}}, \\ S_2^{\lambda} &= P_2^{\lambda_{k_1}} \cup Q_2^{\lambda_{k_2}} \cup R_2^{\lambda_{k_3}}, \ldots, \\ S_k^{\lambda} &= P_k^{\lambda_{k_1}} \cup Q_k^{\lambda_{k_2}} \cup R_k^{\lambda_{k_3}}\}. \end{aligned}$$

which gives $\chi^{\lambda}(\tilde{\mathbb{G}}_1 \cup \tilde{\mathbb{G}}_2 \cup \tilde{\mathbb{G}}_3) = k$ and $\mathcal{L}_{\tilde{\chi}}(k) = \{1-\lambda_t, 1-\lambda_i, 1-\lambda_f\}$

$$\begin{aligned} \mathcal{L}_{\tilde{\chi}}(k) = \{&1 - \max\{\lambda_{t_{(k_1)}}, \lambda_{t_{(k_2)}}, \lambda_{t_{(k_3)}}\}, \\ &1 - \max\{\lambda_{i_{(k_1)}}, \lambda_{i_{(k_2)}}, \lambda_{i_{(k_3)}}\}, \\ &1 - \max\{\lambda_{f_{(k_1)}}, \lambda_{f_{(k_2)}}, \lambda_{f_{(k_3)}}\}\}. \end{aligned}$$

Thus, $\mathcal{L}_{\tilde{\chi}}(k) = \min\{\mathcal{L}_{\tilde{\chi}_1}(k), \mathcal{L}_{\tilde{\chi}_2}(k), \mathcal{L}_{\tilde{\chi}_3}(k)\}$.

For $\min\{m_1, m_2, m_3\} < k \le \max\{m_1, m_2, m_3\}$

Without loss of generality, assume that $m_1 > m_3 > m_2$. Two subcases are being taken into consideration, which are:

1. Maximum clique of underlying graph $(\mathcal{G}_1^* \cup \mathcal{G}_2^* \cup \mathcal{G}_3^*)$ is contained in $\mathcal{G}_1^*$. In this case, there exist $(\lambda_{t_1}, \lambda_{i_1}, \lambda_{f_1}) \in [0,1]$ such that we can construct a partition $A = \{A_1^{\lambda_1} = P_1^{\lambda_1} \cup \{v_1\} \cup \{w_1\}, A_2^{\lambda_1} = P_2^{\lambda_1} \cup \{v_2\} \cup \{w_2\}, \ldots, A_{m_2}^{\lambda_1} = P_{m_2}^{\lambda_1} \cup \{v_{m_2}\} \cup \{w_{m_2}\}, A_{m_2+1}^{\lambda_1} = P_{m_2+1}^{\lambda_1} \cup \{w_{m_2+1}\}, \ldots, A_{m_3}^{\lambda_1} = P_{m_3}^{\lambda_1} \cup \{w_{m_3}\}, A_{m_3+1}^{\lambda_1} = P_{m_3+1}^{\lambda_1}, \ldots, A_k^{\lambda_1} = P_k^{\lambda_1}\}$ on ϑ=$\vartheta_1 \cup \vartheta_2 \cup \vartheta_3$ which gives $\chi^{\lambda}(\tilde{\mathbb{G}})$ = k and $\mathcal{L}_{\tilde{\chi}}(k) = \{1-\lambda_{t_1}, 1-\lambda_{i_1}, 1-\lambda_{f_1}\}$.

Table 5: Partitions on ϑ & λ-$\mathcal{CN}$s of $\tilde{\mathbb{G}}$.

λ	Partitions on ϑ	$\chi^{\lambda}(\tilde{\mathbb{G}})$
(0,1,1)	$\{(AB, BC, DC), (AC), (DB)\}$	3
(0.3,0.1,0.1)	$\{(AB, DC), (AC), (DB, BC)\}$	3
(0.4,0.3,0.2)	$\{(AB, BC, DC), (AC, DB)\}$	2
(0.5,0.3,0.2)	$\{(AB, DC, AC), (BC, DB)\}$	2
(0.8,0.4,0.3)	$\{(AB, BC, DC, DB), (AC)\}$	2
(0.9,0.5,0.6)	$\{(AB, BC, DC, AC, DB)\}$	1

2. Maximum clique of underlying graph $(\mathcal{G}_1^* \cup \mathcal{G}_2^* \cup \mathcal{G}_3^*)$ is contained in $\mathcal{G}_2^*$ or $\mathcal{G}_3^*$. Also by assumption, we have $\max\{m_1, m_2, m_3\} = m_1$ & $\min\{m_1, m_2, m_3\} = m_3$. In this case, we obtain $\mathcal{L}_{\tilde{\chi}}(k) = (1, 0, 0) = \mathcal{L}_{\tilde{\chi}_1}(k) = \mathcal{L}_{\tilde{\chi}_2}(k) = \mathcal{L}_{\tilde{\chi}_3}(k)$ for $\min\{m_1, m_2, m_3\} < k \leq \max\{m_1, m_2, m_3\}$

For $\max\{m_1, m_2, m_3\} < k \leq m = m_1 + m_2 + m_3$

Since $m_1 = \max\{m_1, m_2, m_3\}$, we obtain $\mathcal{L}_{\tilde{\chi}}(m_1) = 1$. It follows from Lemma 3.1 that, $\mathcal{L}_{\tilde{\chi}}(i) = \mathcal{L}_{\tilde{\chi}}(j) = 1$ for any i, j with $m_1 \leq i \leq j \leq m$.

$\therefore$ If we consider $\max\{m_1, m_2, m_3\} = m_2$ or m_3, we will get the result in similar way. □

Remark 3.3. Let $\tilde{\mathbb{G}}_1(\vartheta_1, \tilde{\xi}_1)$ and $\tilde{\mathbb{G}}_2(\vartheta_2, \tilde{\xi}_2)$ be two $\mathcal{SVNG}$s. If $\tilde{\mathbb{G}}_1 \subseteq \tilde{\mathbb{G}}_2$, then the union $\tilde{\mathbb{G}} = \tilde{\mathbb{G}}_1 \cup \tilde{\mathbb{G}}_2 = \tilde{\mathbb{G}}_2$. Therefore, the neutrosophic $\mathcal{CN}$ of union $\tilde{\mathbb{G}} = \tilde{\mathbb{G}}_1 \cup \tilde{\mathbb{G}}_2$ is $\tilde{\chi}(\tilde{\mathbb{G}}) = \{(k, \mathcal{L}_{\tilde{\chi}}(k))\}$, where $\mathcal{L}_{\tilde{\chi}}(k) = \mathcal{L}_{\tilde{\chi}_2}(k)$, for $1 \leq k \leq n = |\vartheta_2|$.

Remark 3.4. Let χ_1, χ_2, and χ_3 be the $\mathcal{CN}$s of the crisp graphs $\mathcal{G}_1^*$, $\mathcal{G}_2^*$, and $\mathcal{G}_3^*$, respectively. Set $M = \max\{\chi_1, \chi_2, \chi_3\}$. If the three graphs admit compatible proper colorings with a common color set of size M (equivalently, if their union admits a proper M-coloring), then $\chi(\mathcal{G}_1^* \cup \mathcal{G}_2^* \cup \mathcal{G}_3^*) = M$. Without this compatibility condition, the equality need not hold.

4. An application

In this section, we explore how the chromatic number of the combined SVNGs can be utilized to determine the optimal number of phases for an integrated traffic-light system. The determination is carried out using three distinct approaches based on the fundamental set and independent vertex set. The proposed model integrates three consecutive traffic intersections into a unified signal control system with the objective of reducing overall cycle time, minimizing traffic congestion, and improving traffic-flow efficiency.

For the purpose of demonstrating the proposed methodology, the traffic-flow data and conflict relationships considered in this study are based on a representative urban traffic scenario. The traffic movements and their corresponding neutrosophic edge values are derived from typical vehicle-flow interactions and conflict patterns observed at signalized intersections. These assumptions are intended to reflect realistic traffic conditions while providing a suitable framework for illustrating the applicability of the proposed SVNG coloring model.

Why graph coloring is suitable for traffic-light control. Graph coloring provides an effective mathematical framework for traffic-signal design because it naturally models conflict relationships among traffic movements. In the proposed representation, each vertex corresponds to a traffic movement, whereas an edge indicates that two movements are conflicting and therefore cannot receive a green signal simultaneously. Assigning different colors to adjacent vertices ensures that conflicting traffic movements are placed in different signal phases. As a result, each color class represents a group of compatible traffic movements that can operate safely at the same time. Consequently, the chromatic number of the graph corresponds to the minimum number of signal phases required to manage all traffic movements without conflicts. This direct relationship makes graph coloring a suitable and efficient tool for traffic-light scheduling and traffic-conflict management.

Selection of traffic-flow thresholds. The traffic-flow intervals $[0, 440]$, $[400, 800]$, and $[760, 1200]$ were selected as representative ranges for low, medium, and high traffic conditions, respectively. The overlapping regions between adjacent intervals were intentionally introduced to capture the uncertainty associated with traffic-flow classification near category boundaries. Consequently, traffic volumes close to the transition points may simultaneously exhibit characteristics of two neighboring traffic categories.

These thresholds are employed solely for illustrative purposes in the present case study and do not represent fixed transportation standards. In practical applications, the interval boundaries may be calibrated using field observations, transportation guidelines, roadway capacities, historical traffic-flow records, or expert assessments. Furthermore, the proposed neutrosophic graph-coloring framework is independent of the particular threshold values adopted. Any alternative membership-function construction or threshold selection can be incorporated without affecting the theoretical results developed in this study.

The practical significance of the proposed approach lies in its ability to handle uncertainty and indeterminacy in traffic systems. In real-world environments, traffic conditions are often influenced by fluctuating vehicle densities, driver behavior, weather conditions, road maintenance activities, and unexpected incidents. Traditional graph-coloring models generally assume deterministic relationships between traffic movements, whereas the proposed SVNG framework incorporates truth, indeterminacy, and falsity membership degrees to represent uncertain traffic conflicts more effectively.

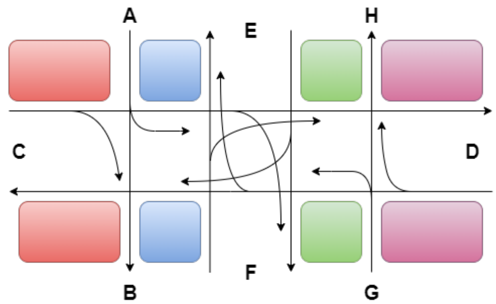

Figure 4: Traffic lights at three intersections.

By modeling traffic movements as vertices and conflict relationships as neutrosophic edges, the chromatic number corresponds to the minimum number of signal phases required to ensure safe and conflict-free traffic operation. Consequently, the proposed method can assist traffic engineers in designing efficient signal plans, reducing vehicle waiting times, improving intersection throughput, and enhancing road safety. Furthermore, the integrated traffic-light system facilitates better coordination among adjacent intersections, thereby reducing stop-and-go movements, fuel consumption, travel delays, and environmental emissions.

The proposed framework may also be extended to intelligent transportation systems, adaptive traffic signal control, smart-city traffic management, and urban mobility planning, where uncertain and dynamic traffic information must be incorporated into the decision-making process.

- In a phase, traffic movements receive a green light assigned to a particular combination during a signal cycle segment.
- Traffic flow typically measures the number of vehicles passing through a specific point on a roadway within a specified time period, usually in vehicles per hour.

Let's examine a four-way intersection (also known as a crossroads) on three intersections as illustrated in Figure 4. On the first (left side) intersection, there are four approaches: A (north), B (south), C (west), and D (east). Similarly, on the second (center) intersection, there are four approaches: E, F, C, and D. Also, on the third (right side) intersection, there are four approaches: H, G, C, and D. As a result, traffic movements occur in various different directions, including AB, CD, DC, AD, CB, EF, FE, CF, DE, EC, FD, GC, GH and DH. Notably, some routes are compatible with each other, such as AB and FE, CB and GH etc., whereas others, such as CF and DE, GH and DC, are incompatible. The union of SVNGs is a representation of the three signalized intersections. When examining traffic flow, it is important to note that each vertex symbolizes the movement of vehicles from one side to the other. When two vertices indicate traffic motions that are in conflict with each other, it is necessary to connect them by an edge. The presence of a membership degree linked to a neutrosophic edge indicates the lack of compatibility between two vertices. This incompatibility suggests the potential for collisions involving vehicles from different streams of traffic. At first, we categorize traffic flow data into three levels of neutrosophic sets: low, medium, high flows. Now, let's explore the traffic flow data presented in the provided Table 6. The notation $\mathscr{L}$, $\mathscr{M}$, and $\mathscr{H}$ correspond to low, medium, and high, respectively. In traffic movements, the number of vehicles per hour is denoted by the symbol $\mathscr{N}$. In the context of traffic flow analysis, we consider three distinct SVNSs based on traffic volume as follows:

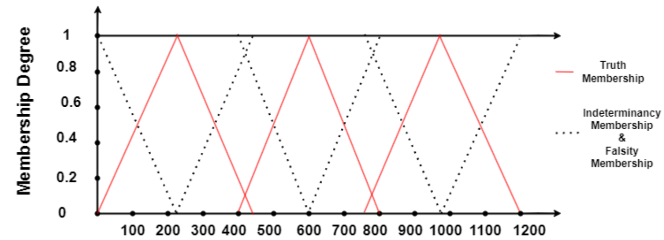

Figure 5: Membership functions of different traffic flows.

- The low traffic flow is depicted by a SVN triangular membership function over the interval of [0, 440].
- The medium traffic flow is depicted by a SVN triangular membership function over the interval of [400, 800].
- The high traffic flow is depicted by a SVN triangular membership function over the interval of [760, 1200].

In the proposed traffic model, each vertex represents a traffic movement (vehicle stream) from one approach of an intersection to another, such as AB, CD, or EF. Therefore, vertices do not represent roads, lanes, or intersection approaches themselves, but rather the directional movement of vehicles between approaches. An edge is introduced between two vertices whenever the corresponding traffic movements are incompatible and cannot be executed simultaneously without creating a traffic conflict. The neutrosophic edge value quantifies the degree of conflict, uncertainty, and non-conflict between the two traffic movements. Under this representation, graph coloring partitions the traffic movements into compatible groups, where each color corresponds to a signal phase. Consequently, the chromatic number represents the minimum number of signal phases required for safe and efficient traffic operation.

The neutrosophic values listed in Table 6 are the final values used throughout all subsequent edge construction, score-function evaluation, and chromatic-number calculations. The process of neutrosophication being applied to the traffic flow data in Table 6 is depicted in Figure 5. By representing the degree of membership of the edge, we may enhance our comprehension of the incompatibility between two traffic flows. The next phase involves determining the membership degrees for each edge (degree of conflict) using the given guideline.

1. If there is no conflict between the traffic movements PQ and RS, indicating that they can proceed simultaneously, then there is no edge between them. The neutrosophic edge is defined by a membership degree of (0,1,1).

Table 6: Data of traffic flows (vehicles/hour).

ϑ	$\mathscr{N}$	Low ($\mathscr{L}$)	Medium ($\mathscr{M}$)	High ($\mathscr{H}$)
AB	465		$(0.33, 0.67, 0.67)$	
CD	1090			$(0.50, 0.50, 0.50)$
DC	425			$(0.13, 0.87, 0.87)$
AD	876			$(0.53, 0.47, 0.47)$
CB	576		$(0.88, 0.12, 0.12)$	
EF	893			$(0.60, 0.40, 0.40)$
FD	961			$(0.91, 0.09, 0.09)$
FE	742		$(0.29, 0.71, 0.71)$	
CF	658		$(0.71, 0.29, 0.29)$	
DE	248	$(0.87, 0.13, 0.13)$		
EC	253	$(0.85, 0.15, 0.15)$		
GC	472		$(0.36, 0.64, 0.64)$	
GH	361	$(0.36, 0.64, 0.64)$		
DH	392	$(0.22, 0.78, 0.78)$		

Table 7: Score values of the traffic movements.

Traffic movement	SVNN (T, I, F)	Score
AB	$(0.33, 0.67, 0.67)$	0.33
CD	$(0.50, 0.50, 0.50)$	0.50
DC	$(0.13, 0.87, 0.87)$	0.13
AD	$(0.53, 0.47, 0.47)$	0.53
CB	$(0.88, 0.12, 0.12)$	0.88
EF	$(0.60, 0.40, 0.40)$	0.60
FD	$(0.91, 0.09, 0.09)$	0.91
FE	$(0.29, 0.71, 0.71)$	0.29
CF	$(0.71, 0.29, 0.29)$	0.71
DE	$(0.87, 0.13, 0.13)$	0.87
EC	$(0.85, 0.15, 0.15)$	0.85
GC	$(0.36, 0.64, 0.64)$	0.36
GH	$(0.36, 0.64, 0.64)$	0.36
DH	$(0.22, 0.78, 0.78)$	0.22

2. If the traffic movements PQ and RS are incompatible (in conflict), meaning they cannot occur simultaneously , we establish an edge (PQ, RS). Furthermore, we determine the membership degree of the neutrosophic edge (PQ, RS) by selecting the maximum value from the membership degrees of PQ and RS.

The maximum value of two $\mathcal{SVNN}s$ can be determined by applying Definition-2.3. The score function values for all vertices are listed in Table 7. By using the provided rule, we can model the traffic flows on the first, second and third intersections in Figure 4 as three SVNGs $\tilde{\mathbb{G}}_1(\vartheta_1, \tilde{\xi}_1)$, $\tilde{\mathbb{G}}_2(\vartheta_2, \tilde{\xi}_2)$ and $\tilde{\mathbb{G}}_3(\vartheta_3, \tilde{\xi}_3)$ respectively. Here, the vertex sets are delineated as follows:

- For $\tilde{\mathbb{G}}_1$, the vertex set is

$$\vartheta_1 = \{AB, CB, AD, CD, DC, CF, EC, GC\}.$$

- For $\tilde{\mathbb{G}}_2$, the vertex set is

$$\vartheta_2 = \{EF, FE, CD, DC, AD, CF, DE, EC, FD, GC\}.$$

- For $\tilde{\mathbb{G}}_3$, the vertex set is

$$\vartheta_3 = \{CD, DC, AD, DE, FD, GC, GH, DH\}.$$

Tables 8 and 9 display the membership degrees of edges within the neutrosophic edge set $\tilde{\xi}$. They present the neutrosophic edge relationships of the traffic network. For readability, the complete edge set is divided into two parts, where each entry (T, I, F) denotes the truth-membership, indeterminacy-membership, and falsity-membership degrees associated with the corresponding pair of traffic movements. The edge values in Table 9 are computed directly from the neutrosophic traffic-flow values reported in Table 6 using the proposed construction rules.

4.1. Method 1: Using the fundamental set

From the given Tables 8 and 9, the fundamental set A of $\mathcal{SVNG}$ $\tilde{\mathbb{G}}$ can be acquired,

$$A = \{(0.29, 0.71, 0.71), (0.33, 0.67, 0.67), (0.36, 0.64, 0.64), (0.5, 0.5, 0.5), (0.53, 0.47, 0.47), (0.6, 0.4, 0.4), (0.71, 0.29, 0.29), (0.85, 0.15, 0.15), (0.87, 0.13, 0.13), (0.88, 0.12, 0.12), (0.91, 0.09, 0.09)\}. \quad (1)$$

The $\mathcal{SVNG}s$ $\tilde{\mathbb{G}}_1(\vartheta_1, \tilde{\xi}_1)$, $\tilde{\mathbb{G}}_2(\vartheta_2, \tilde{\xi}_2)$ and $\tilde{\mathbb{G}}_3(\vartheta_3, \tilde{\xi}_3)$ are shown in the following figures.

To clarify the construction of the neutrosophic edge values reported in Tables 8 and 9, we provide a representative example.

Consider the traffic movements AB and CB. From Table 6, the neutrosophic representations of these traffic flows are

$$AB = (0.33, 0.67, 0.67),$$

and

$$CB = (0.88, 0.12, 0.12).$$

Table 8: Neutrosophic edge sets (Part 1).

M	AB	CD	DC	AD	CB	EF	FD
AB	–	(0.5,0.5,0.5)	(0.33,0.67,0.67)	–	(0.88,0.12,0.12)	–	–
CD	(0.5,0.5,0.5)	–	–	(0.53,0.47,0.47)	–	(0.6,0.4,0.4)	(0.91,0.09,0.09)
DC	(0.33,0.67,0.67)	–	–	–	(0.88,0.12,0.12)	(0.6,0.4,0.4)	(0.91,0.09,0.09)
AD	–	(0.53,0.47,0.47)	–	–	–	(0.6,0.4,0.4)	(0.91,0.09,0.09)
CB	(0.88,0.12,0.12)	–	(0.88,0.12,0.12)	–	–	–	–
EF	–	(0.6,0.4,0.4)	(0.6,0.4,0.4)	(0.6,0.4,0.4)	–	–	(0.91,0.09,0.09)
FD	–	(0.91,0.09,0.09)	(0.91,0.09,0.09)	(0.91,0.09,0.09)	–	(0.91,0.09,0.09)	–
FE	–	(0.5,0.5,0.5)	(0.29,0.71,0.71)	(0.53,0.47,0.47)	–	–	–
CF	(0.71,0.29,0.29)	–	(0.71,0.29,0.29)	(0.71,0.29,0.29)	–	(0.71,0.29,0.29)	(0.91,0.09,0.09)
DE	–	(0.87,0.13,0.13)	–	(0.87,0.13,0.13)	–	(0.87,0.13,0.13)	(0.91,0.09,0.09)
EC	(0.85,0.15,0.15)	(0.85,0.15,0.15)	(0.85,0.15,0.15)	(0.85,0.15,0.15)	(0.85,0.15,0.15)	–	(0.91,0.09,0.09)
GC	(0.36,0.64,0.64)	–	(0.36,0.64,0.64)	–	(0.88,0.12,0.12)	(0.6,0.4,0.4)	(0.91,0.09,0.09)
GH	–	(0.5,0.5,0.5)	(0.36,0.64,0.64)	(0.53,0.47,0.47)	–	–	(0.91,0.09,0.09)
DH	–	(0.5,0.5,0.5)	–	(0.53,0.47,0.47)	–	–	(0.91,0.09,0.09)

Table 9: Neutrosophic edge sets (Part 2).

M	FE	CF	DE	EC	GC	GH	DH
AB	–	(0.71,0.29,0.29)	–	(0.85,0.15,0.15)	(0.36,0.64,0.64)	–	–
CD	(0.50,0.50,0.50)	–	(0.87,0.13,0.13)	(0.85,0.15,0.15)	–	(0.50,0.50,0.50)	(0.50,0.50,0.50)
DC	(0.29,0.71,0.71)	(0.71,0.29,0.29)	–	(0.85,0.15,0.15)	(0.36,0.64,0.64)	(0.36,0.64,0.64)	–
AD	(0.53,0.47,0.47)	(0.71,0.29,0.29)	(0.87,0.13,0.13)	(0.85,0.15,0.15)	–	(0.53,0.47,0.47)	(0.53,0.47,0.47)
CB	–	–	–	(0.85,0.15,0.15)	(0.88,0.12,0.12)	–	–
EF	–	(0.71,0.29,0.29)	(0.87,0.13,0.13)	–	(0.60,0.40,0.40)	–	–
FD	–	(0.91,0.09,0.09)	(0.91,0.09,0.09)	(0.91,0.09,0.09)	(0.91,0.09,0.09)	(0.91,0.09,0.09)	(0.91,0.09,0.09)
FE	–	(0.71,0.29,0.29)	(0.87,0.13,0.13)	(0.85,0.15,0.15)	(0.36,0.64,0.64)	–	–
CF	(0.71,0.29,0.29)	–	(0.87,0.13,0.13)	(0.85,0.15,0.15)	(0.71,0.29,0.29)	–	–
DE	(0.87,0.13,0.13)	(0.87,0.13,0.13)	–	(0.87,0.13,0.13)	(0.87,0.13,0.13)	(0.87,0.13,0.13)	–
EC	(0.85,0.15,0.15)	(0.85,0.15,0.15)	(0.87,0.13,0.13)	–	(0.85,0.15,0.15)	–	–
GC	(0.36,0.64,0.64)	(0.71,0.29,0.29)	(0.87,0.13,0.13)	(0.85,0.15,0.15)	–	–	–
GH	–	–	(0.87,0.13,0.13)	–	–	–	(0.36,0.64,0.64)
DH	–	–	–	–	–	(0.36,0.64,0.64)	–

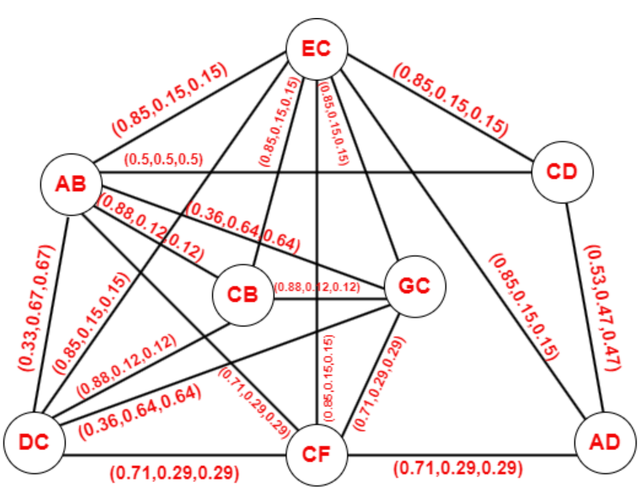

Figure 6: $\tilde{\mathbb{G}}_1(\vartheta_1, \tilde{\xi}_1)$.

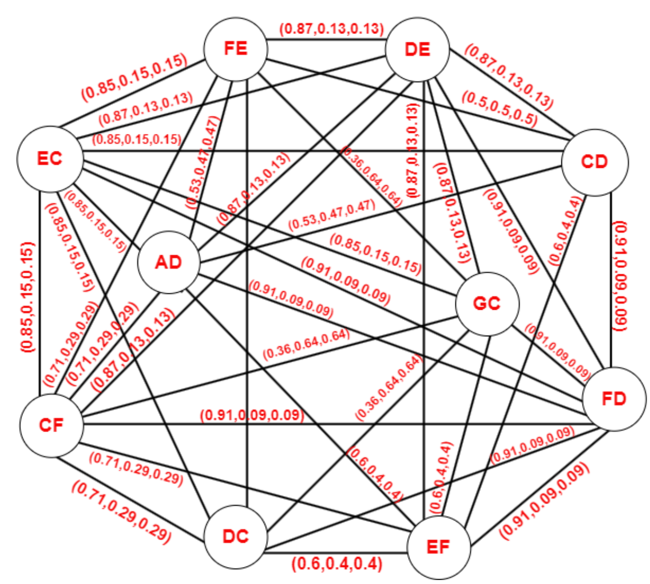

Figure 7: $\tilde{\mathbb{G}}_2(\vartheta_2, \tilde{\xi}_2)$.

The corresponding score-function values are obtained from Definition 2.3 and are listed in Table 7 as

$$S(AB) = 0.33, \qquad S(CB) = 0.88.$$

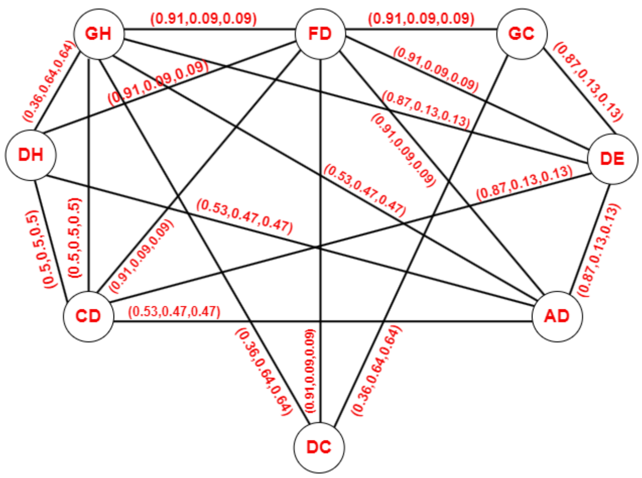

Figure 8: $\tilde{\mathbb{G}}_3(\vartheta_3, \tilde{\xi}_3)$.

Since the traffic movements AB and CB are incompatible and cannot occur simultaneously, an edge is established between the corresponding vertices.

According to the proposed rule, the neutrosophic value of a conflicting edge is determined by selecting the maximum neutrosophic assessment of the two associated traffic movements. Since

$$S(CB) = 0.88 > S(AB) = 0.33,$$

the edge membership value is assigned as

$$(AB, CB) = (0.88, 0.12, 0.12).$$

Similarly, consider the conflicting traffic movements CD and EF with neutrosophic values

$$CD = (0.50, 0.50, 0.50),$$

and

$$EF = (0.60, 0.40, 0.40).$$

Since

$$S(EF) = 0.60 > S(CD) = 0.50,$$

the corresponding neutrosophic edge value is

$$(CD, EF) = (0.60, 0.40, 0.40).$$

The same procedure is applied to all conflicting traffic movements to construct the neutrosophic edge sets reported in Tables 8 and 9. If two traffic movements are compatible and can safely operate simultaneously, no edge is introduced between the corresponding vertices. The SVNGs shown in Figures 6–8 represent the traffic-flow structures of three different junctions. In these graphs, vertices correspond to traffic movements, while neutrosophic edge values describe the associated truth, indeterminacy, and falsity degrees of conflict between movements. These SVNGs serve as the basis for determining the neutrosophic chromatic numbers and analyzing traffic signal scheduling under uncertain conditions. NG coloring can be accomplished through various methods. Using any chromatic algorithm, it is easy to determine the chromatic numbers of the SVNGs $\tilde{\mathbb{G}}_1$, $\tilde{\mathbb{G}}_2$ and $\tilde{\mathbb{G}}_3$. Specifically, the $\mathcal{CN}$ of SVNGs $\tilde{\mathbb{G}}_1$, $\tilde{\mathbb{G}}_2$ and $\tilde{\mathbb{G}}_3$ are determined by using Definition-2.8 are as follows: $\chi(\mathbb{G}_1) = 5; \chi(\mathbb{G}_2) = 5; \chi(\mathbb{G}_3) = 5$. Moreover, the integration of three intersections depicted in Figure 4 can be represented through an integrated traffic light system, achieved by combining the SVNGs $\tilde{\mathbb{G}} = \tilde{\mathbb{G}}_1 \cup \tilde{\mathbb{G}}_2 \cup \tilde{\mathbb{G}}_3$ by using Definition-3.2, as shown in Figure 9. The $\mathcal{CN}$ of the union shown in Figure-9 can be determined using the following manner.

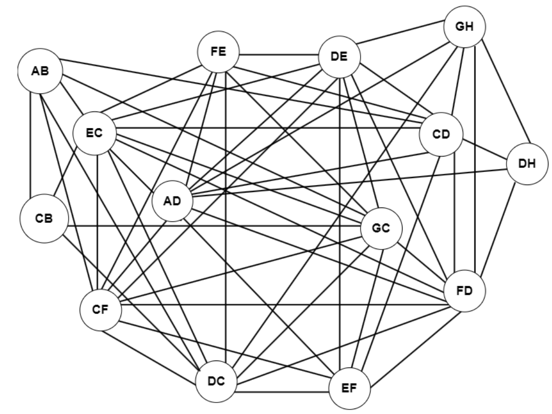

Figure 9: $\tilde{\mathbb{G}} = \tilde{\mathbb{G}}_1 \cup \tilde{\mathbb{G}}_2 \cup \tilde{\mathbb{G}}_3$.

$$\begin{aligned}\chi(\tilde{\mathbb{G}}) &= \max\{\chi(G_{\alpha_i,\beta_i,\gamma_i}) \mid \alpha_i, \beta_i, \gamma_i \in A\} \\ &= \chi(\tilde{\mathbb{G}}_1 \cup \tilde{\mathbb{G}}_2 \cup \tilde{\mathbb{G}}_3) \\ &= 5..\end{aligned}$$

The $\mathcal{CN}$ of crisp graphs, denoted as $\chi(G_{\alpha_i,\beta_i,\gamma_i}) = \text{k}$, can be elucidated as follows: The value k signifies the quantity of phases required in the integrated system, while the membership degree $\alpha_i, \beta_i, \gamma_i$ indicates the probability of potential traffic incidents occurring when utilizing these k phases. Table 10 displays specific arrangements of traffic flows for the SVNG $\tilde{\mathbb{G}}(\vartheta, \tilde{\xi})$ based on the $\mathcal{CN}$ k of the $\alpha_i, \beta_i, \gamma_i$-cut graph shown in Figure 4. Based on the $\mathcal{CN}$, k of the strong $\alpha_i, \beta_i, \gamma_i$ -cut graph for the SVNG $\tilde{\mathbb{G}}(\vartheta, \tilde{\xi})$, traffic flows illustrated in Figure 4 might be organized into specific configurations, as shown in Table 11.

4.2. Method 2: Using the neutrosophic independent vertex set

A traffic light system on three intersections in Figure 4 can be modelled as three SVNGs $\tilde{\mathbb{G}}_1(\vartheta_1, \tilde{\xi}_1)$, $\tilde{\mathbb{G}}_2(\vartheta_2, \tilde{\xi}_2)$, and $\tilde{\mathbb{G}}_3(\vartheta_3, \tilde{\xi}_3)$, respectively, where the vertex sets are:

$$\begin{aligned}\vartheta_1 &= \{AB, CB, AD, CD, DC, CF, EC, GC\}, \\ \vartheta_2 &= \{EF, FE, CD, DC, AD, CF, DE, EC, FD, GC\}, \\ \vartheta_3 &= \{CD, DC, AD, DE, FD, GC, GH, DH\}.\end{aligned}$$

Membership degrees of edges in neutrosophic edge set $\tilde{\xi}_1, \tilde{\xi}_2$ and $\tilde{\xi}_3$. The SVNGs $\tilde{\mathbb{G}}_1(\vartheta_1, \tilde{\xi}_1)$, $\tilde{\mathbb{G}}_2(\vartheta_2, \tilde{\xi}_2)$ and $\tilde{\mathbb{G}}_3(\vartheta_3, \tilde{\xi}_3)$ are depicted in Figures 6, 7 and 8 respectively. Table-12 presents

Table 10: Arrangements using α, β, γ-cuts.

$\alpha_i, \beta_i, \gamma_i$	k	Arrangements
(0.29,0.71,0.71)	5	$\{AB, FE, FD\}, \{EC, EF, GH\}, \{CB, CF, CD\}, \{DE, DH, DC\}, \{AD, GC\}$
(0.33,0.67,0.67)	5	$\{AB, FE, FD\}, \{EC, EF, GH\}, \{CB, CF, CD\}, \{DE, DH, DC\}, \{AD, GC\}$
(0.36,0.64,0.64)	5	$\{FE, FD\}, \{EC, EF, GH\}, \{CB, CF, CD\}, \{DE, DH, DC, AB\}, \{AD, GC\}$
(0.5,0.5,0.5)	5	$\{FE, FD\}, \{EC, EF, GH, DH\}, \{CB, CF, CD\}, \{DE, AB\}, \{AD, GC, DC\}$
(0.53,0.47,0.47)	5	$\{FE, FD\}, \{EC, EF, GH, DH\}, \{CB, CF, CD\}, \{DE, AB\}, \{AD, GC, DC\}$
(0.6,0.4,0.4)	5	$\{FE, FD\}, \{EC, EF\}, \{CB, CF, CD\}, \{DE, AB\}, \{AD, GC, DC, DH, GH\}$
(0.71,0.29,0.29)	5	$\{FE, FD\}, \{EC\}, \{CB, CF, CD\}, \{DE, AB\}, \{AD, GC, DC, DH, GH, EF\}$
(0.85,0.15,0.15)	4	$\{FE, FD, CB\}, \{EC\}, \{DE, AB\}, \{AD, GC, DC, DH, GH, EF, CF, CD\}$
(0.87,0.13,0.13)	3	$\{FE, FD, CB\}, \{DE\}, \{AB, EC, AD, GC, DC, DH, GH, EF, CF, CD\}$
(0.88,0.12,0.12)	2	$\{FD, CB\}, \{FE, AB, EC, AD, DE, GC, DC, DH, GH, EF, CF, CD\}$
(0.91,0.09,0.09)	2	$\{FD\}, \{FE, AB, EC, CB, AD, DE, GC, DC, DH, GH, EF, CF, CD\}$

Table 11: Arrangements using strong α, β, γ-cuts.

$\alpha_i, \beta_i, \gamma_i$	k	Arrangements
(0.29,0.71,0.71)	5	$\{AB, FE, FD\}, \{EC, EF, GH\}, \{CB, CF, CD\}, \{DE, DH, DC\}, \{AD, GC\}$
(0.33,0.67,0.67)	5	$\{FE, FD\}, \{EC, EF, GH\}, \{CB, CF, CD\}, \{DE, DH, DC, AB\}, \{AD, GC\}$
(0.36,0.64,0.64)	5	$\{FE, FD\}, \{EC, EF, GH, DH\}, \{CB, CF, CD\}, \{DE, AB\}, \{AD, GC, DC\}$
(0.5,0.5,0.5)	5	$\{FE, FD\}, \{EC, EF, GH, DH\}, \{CB, CF, CD\}, \{DE, AB\}, \{AD, GC, DC\}$
(0.53,0.47,0.47)	5	$\{FE, FD\}, \{EC, EF\}, \{CB, CF, CD\}, \{DE, AB\}, \{AD, GC, DC, DH, GH\}$
(0.6,0.4,0.4)	5	$\{FE, FD\}, \{EC\}, \{CB, CF, CD\}, \{DE, AB\}, \{AD, GC, DC, DH, GH, EF\}$
(0.71,0.29,0.29)	4	$\{FE, FD, CB\}, \{EC\}, \{DE, AB\}, \{AD, GC, DC, DH, GH, EF, CF, CD\}$
(0.85,0.15,0.15)	3	$\{FE, FD, CB\}, \{DE\}, \{AB, EC, AD, GC, DC, DH, GH, EF, CF, CD\}$
(0.87,0.13,0.13)	2	$\{FD, CB\}, \{FE, AB, EC, AD, DE, GC, DC, DH, GH, EF, CF, CD\}$
(0.88,0.12,0.12)	2	$\{FD\}, \{FE, AB, EC, CB, AD, DE, GC, DC, DH, GH, EF, CF, CD\}$
(0.91,0.09,0.09)	1	$\{AB, FE, FD, EC, EF, GH, CB, CF, CD, DE, DH, DC, AD, GC\}$

Table 12: λ-chromatic numbers of $\tilde{\mathbb{G}}_1$.

$\lambda_t, \lambda_i, \lambda_f$	$\chi^\lambda(\tilde{\mathbb{G}}_1)$	Partitions on ϑ_1
(0,1,1)	5	$\{AB\}, \{EC\}, \{CB, CF\}, \{AD, DC\}, \{CD, GC\}$
(0.33,0.67,0.67)	4	$\{EC\}, \{CB, CF\}, \{AB, AD, DC\}, \{CD, GC\}$
(0.36,0.64,0.64)	3	$\{EC\}, \{CB, CF, CD\}, \{AB, AD, DC, GC\}$
(0.5,0.5,0.5)	3	$\{EC\}, \{CB, CF, CD\}, \{AB, AD, DC, GC\}$
(0.53,0.47,0.47)	3	$\{EC\}, \{CB, CF\}, \{AB, AD, DC, GC, CD\}$
(0.71,0.29,0.29)	3	$\{EC\}, \{CB\}, \{AB, AD, DC, GC, CD, CF\}$
(0.85,0.15,0.15)	2	$\{CB\}, \{AB, AD, DC, GC, CD, CF, EC\}$
(0.88,0.12,0.12)	1	$\{CB, AB, AD, DC, GC, CD, CF, EC\}$

several partitions of ϑ & λ-$\mathcal{CN}$s of $\tilde{\mathbb{G}}_1$ by utilizing Definition-3.6. The neutrosophic $\mathcal{CN}$ of $\tilde{\mathbb{G}}_1$ can be calculated using Definition 3.7 and Table 12.

$$\tilde{\chi}(\tilde{\mathbb{G}}_1) = \{(1, (0.12, 0.88, 0.88)), (2, (0.15, 0.85, 0.85)), (3, (0.64, 0.36, 0.36)), (4, (0.67, 0.33, 0.33)), (5, (1, 0, 0)), (6, (1, 0, 0)), (7, (1, 0, 0)), (8, (1, 0, 0))\}. \quad (2)$$

Similarly, λ-$\mathcal{CN}$s and neutrosophic $\mathcal{CN}$ of $\tilde{\mathbb{G}}_2$ & $\tilde{\mathbb{G}}_3$ are obtained and presented in the following Tables 13 , 14.
Neutrosophic chromatic number of $\tilde{\mathbb{G}}_2$ as follows:

$$\tilde{\chi}(\tilde{\mathbb{G}}_2) = \{(1, (0.09, 0.91, 0.91)), (2, (0.13, 0.87, 0.87)), (3, (0.15, 0.85, 0.85)), (4, (0.29, 0.71, 0.71)), (5, (1, 0, 0)), (6, (1, 0, 0)), (7, (1, 0, 0)), (8, (1, 0, 0)), (9, (1, 0, 0)), (10, (1, 0, 0))\}. \quad (3)$$

Neutrosophic chromatic number of $\tilde{\mathbb{G}}_3$ as follows:

$$\tilde{\chi}(\tilde{\mathbb{G}}_3) = \{(1, (0.09, 0.91, 0.91)), (2, (0.13, 0.87, 0.87)), (3, (0.47, 0.53, 0.53)), (4, (0.5, 0.5, 0.5)), (5, (1, 0, 0)), (6, (1, 0, 0)), (7, (1, 0, 0)), (8, (1, 0, 0))\}. \quad (4)$$

Moreover, the integration of three intersections visualized in Figure 4, can be represented by an integrated traffic light system that utilizes the union of SVNGs $\tilde{\mathbb{G}} = \tilde{\mathbb{G}}_1 \cup \tilde{\mathbb{G}}_2 \cup \tilde{\mathbb{G}}_3$, as illustrated in Figure 9. Because the three vertex sets overlap,

Table 13: λ-chromatic numbers of $\tilde{\mathbb{G}}_2$.

$\lambda_t, \lambda_i, \lambda_f$	$\chi^\lambda(\tilde{\mathbb{G}}_2)$	Partitions on ϑ_2
(0,1,1)	5	$\{FE, FD\}, \{EC, EF\}, \{CF, CD\}, \{DE, DC\}, \{AD, GC\}$
(0.29,0.71,0.71)	5	$\{FE, FD\}, \{EC, EF\}, \{CF, CD\}, \{DE, DC\}, \{AD, GC\}$
(0.36,0.64,0.64)	5	$\{FE, FD\}, \{EC, EF\}, \{CF, CD\}, \{DE, DC\}, \{AD, GC\}$
(0.5,0.5,0.5)	5	$\{FE, FD\}, \{EC, EF\}, \{CF, CD, GC\}, \{DE, DC\}, \{AD\}$
(0.53,0.47,0.47)	5	$\{FE, FD\}, \{EC, EF\}, \{CF, CD, GC\}, \{DE, DC\}, \{AD\}$
(0.6,0.4,0.4)	5	$\{FE, FD\}, \{EC, EF\}, \{CF, CD, GC\}, \{DE, DC\}, \{AD\}$
(0.71,0.29,0.29)	4	$\{FE, FD\}, \{EC\}, \{CF, CD, GC, EF, AD\}, \{DE, DC\}$
(0.85,0.15,0.15)	3	$\{FE, FD\}, \{EC, CF, CD, GC, EF, AD, DC\}, \{DE\}$
(0.87,0.13,0.13)	2	$\{FD\}, \{EC, CF, CD, GC, EF, AD, DC, FE, DE\}$
(0.91,0.09,0.09)	1	$\{FD, EC, CF, CD, GC, EF, AD, DC, FE, DE\}$

Table 14: λ-chromatic numbers of $\tilde{\mathbb{G}}_3$.

$\lambda_t, \lambda_i, \lambda_f$	$\chi^\lambda(\tilde{\mathbb{G}}_3)$	Partitions on ϑ_3
(0,1,1)	5	$\{FD\}, \{GH\}, \{GC, CD\}, \{DE, DH\}, \{AD, DC\}$
(0.36,0.64,0.64)	5	$\{FD\}, \{GH\}, \{GC, DC, AD\}, \{DE, DH\}, \{CD\}$
(0.5,0.5,0.5)	4	$\{FD\}, \{GH, CD\}, \{GC, DC, AD\}, \{DE, DH\}$
(0.53,0.47,0.47)	3	$\{FD\}, \{GH, CD, GC, DC, AD\}, \{DE, DH\}$
(0.87,0.13,0.13)	2	$\{FD\}, \{GH, CD, GC, DC, AD, DE, DH\}$
(0.91,0.09,0.09)	1	$\{FD, GH, CD, GC, DC, AD, DE, DH\}$

the terminal range of Theorem 3.1 is not directly applicable here. The resulting union has 14 distinct vertices, and its neutrosophic CN is written as follows:

$$\begin{aligned}\tilde{\chi}(\tilde{\mathbb{G}}) = \{&(1, (0.09, 0.91, 0.91)), (2, (0.13, 0.87, 0.87)),\\ &(3, (0.15, 0.85, 0.85)), (4, (0.29, 0.71, 0.71)),\\ &(5, (1, 0, 0)), (6, (1, 0, 0)), (7, (1, 0, 0)), (8, (1, 0, 0)),.\\ &(9, (1, 0, 0)), (10, (1, 0, 0)), (11, (1, 0, 0)),\\ &(12, (1, 0, 0)), (13, (1, 0, 0)), (14, (1, 0, 0)\}.\end{aligned} \tag{5}$$

The neutrosophic CN of the union of SVNGs, denoted as $\tilde{\chi}(\tilde{\mathbb{G}})$, is represented as $\{(k, \mathcal{L}_{\tilde{\chi}}(k))\}$. Here's the interpretation:

- The integrated system requires a certain number of phases, denoted by k.
- The degree of membership $\mathcal{L}_{\tilde{\chi}}(k)$ reflects the possibility of avoiding accidents (degree of safety) when using k phases.

Furthermore, considering the neutrosophic CN from equation 5 and the λ-CNs k, the traffic flows depicted in Figure 4 can be organized into specific patterns, as illustrated in Table 15.

As an illustration, when implementing a system with $k = 2$ phases, a degree of incompatibility of (0.87,0.13,0.13) is attained. In the initial phase, the traffic flow that is allowed to move simultaneously (indicated by a green light) includes CF, EF, GH, CD, DH, DC, AD, GC, AB, EC, FE and DE. In the second phase, CB and FD are permitted. The goal is to achieve an optimal configuration where the level of safety is maximized, and simultaneously, the number of phases is minimized. When $k = 5$, the objective is reached as shown in Figure 10. The allowed traffic movements during the phases are:

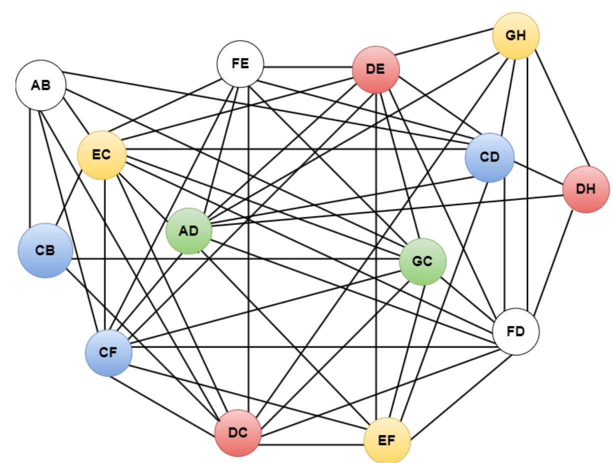

Figure 10: Optimal arrangement.

- AB, FE, and FD in the first phase;
- EC, EF and GH in the second phase;
- CB, CF and CD in the third phase;
- DE, DH and DC in the fourth phase and
- AD and GC in the fifth phase.

This specific arrangement ensures the maximum prevention of traffic incidents. A comparative analysis of α, β, γ-cuts, strong α, β, γ-cuts, and the independent vertex set of an SVNG is presented in Table 16. Tables 15 and 16 show that an optimal arrangement can be obtained using any of the proposed methods because the objective is reached at $k = 5$ in all cases.

Table 15: Arrangement of traffic light using k-phases.

$(\lambda_t, \lambda_i, \lambda_f)$	k	$\mathcal{L}_{\tilde{\chi}}(k)$	Partitions on ϑ
$(0, 1, 1)$	5	$(1, 0, 0)$	$\{AB, FE, FD\}, \{EC, EF, GH\}, \{CB, CF, CD\}, \{DE, DH, DC\}, \{AD, GC\}$
$(0.71, 0.29, 0.29)$	4	$(0.29, 0.71, 0.71)$	$\{AB, DE\}, \{EC\}, \{CB, FE, FD\}, \{CF, EF, GH, CD, DH, DC, AD, GC\}$
$(0.85, 0.15, 0.15)$	3	$(0.15, 0.85, 0.85)$	$\{DE\}, \{CB, FE, FD\}, \{CF, EF, GH, CD, DH, DC, AD, GC, AB, EC\}$
$(0.87, 0.13, 0.13)$	2	$(0.13, 0.87, 0.87)$	$\{CB, FD\}, \{CF, EF, GH, CD, DH, DC, AD, GC, AB, EC, FE, DE\}$
$(0.91, 0.09, 0.09)$	1	$(0.09, 0.91, 0.91)$	$\{CB, FD, CF, EF, GH, CD, DH, DC, AD, GC, AB, EC, FE, DE\}$

Table 16: Comparative analysis of the proposed methods.

k - Phases	$\alpha, \beta, \gamma - cuts$	Strong $\alpha, \beta, \gamma - cuts$	independent vertex set
5	(0.29,0.71,0.71)	(0.29,0.71,0.71)	(0,1,1)
4	(0.85,0.15,0.15)	(0.71,0.29,0.29)	(0.71,0.29,0.29)
3	(0.87,0.13,0.13)	(0.85,0.15,0.15)	(0.85,0.15,0.15)
2	(0.88,0.12,0.12)	(0.87,0.13,0.13)	(0.87,0.13,0.13)
1	-	(0.91,0.09,0.09)	(0.91,0.09,0.09)

Table 17: Comparison of graph-coloring frameworks.

Feature	Classical Graph	Fuzzy Graph	Intuitionistic Fuzzy Graph	single-valued neutrosophic graph
Uncertainty	×	✓	✓	✓
Indeterminacy	×	×	×	✓
Truth membership	×	✓	✓	✓
Non-membership	×	×	✓	✓
Traffic conflict modeling	Low	Med.	Med.	High
Chromatic framework	×	×	×	✓

The strong α, β, γ-cut and independent-vertex-set methods produce more similar k-phase results. The independent-vertex-set method gives the best k-coloring result because the degree of safety is exactly one.

5. Discussion and limitations

The traffic-light application presented in this study is intended primarily as an illustrative example demonstrating the applicability of the proposed SVNG chromatic-number framework under uncertain traffic conditions. The traffic-flow data and conflict relationships were selected to construct a representative traffic scenario and to illustrate the process of modeling traffic movements, conflict relationships, and signal phases within a neutrosophic graph environment.

It should be noted that the present study does not aim to provide a comprehensive operational evaluation of traffic signal performance. Consequently, no simulation experiments, field studies, or comparisons with existing signal-timing methods have been conducted. Similarly, performance indicators such as vehicle delay, queue length, throughput, travel time, fuel consumption, and accident reduction were not considered within the scope of this work.

The primary contribution of this study lies in the development of a novel theoretical framework for neutrosophic graph coloring and its potential application to traffic-signal control problems. Future research may incorporate real-world traffic datasets, microscopic traffic simulations, and comparative analyses with conventional signal-control techniques to assess the practical effectiveness and operational benefits of the proposed approach.

Although the proposed SVNG chromatic-number framework provides a novel mathematical approach for graph coloring under uncertainty, several limitations should be acknowledged. First, the traffic-light application presented in this study is primarily illustrative and is intended to demonstrate the applicability of the proposed framework rather than provide a fully validated traffic-control solution. The traffic-flow data and membership-function parameters were selected for demonstration purposes and may require calibration when applied to real-world traffic systems.

Second, the study does not include simulation experiments, field implementations, or comparisons with existing traffic-signal optimization methods. Consequently, operational performance measures such as vehicle delay, queue length, throughput, fuel consumption, and accident reduction have not been evaluated. Third, the proposed framework has been developed within the setting of single-valued neutrosophic graphs, and its applicability to other neutrosophic graph structures remains an open research problem.

Future research may focus on validating the proposed approach using real-world traffic datasets, conducting simulation-based performance analyses, comparing the framework with existing graph-coloring and traffic-control methods, and extending the proposed chromatic-number concepts to interval-valued, bipolar, picture, spherical, and other advanced neutrosophic graph environments.

5.1. Discussion and comparison of the obtained chromatic numbers

A comparison of the chromatic numbers obtained using the different proposed approaches reveals several important observations. Although the fundamental set approach, strong fundamental set approach, and neutrosophic independent vertex set approach are derived from different perspectives, they all aim to determine the minimum number of colors (signal phases) required to avoid conflicts among traffic movements. The fundamental set approach considers edge relationships based on the specified (α, β, γ) thresholds, whereas the strong fundamental set approach imposes stricter conditions, resulting in a more restrictive graph structure. Consequently, the chromatic numbers obtained from the strong cut approach may differ from those obtained using ordinary cuts due to the reduced number of admissible edges.

On the other hand, the neutrosophic independent vertex set approach determines the chromatic number through the partitioning of mutually non-adjacent traffic movements. This method provides an alternative interpretation of traffic signal grouping and offers additional insight into the structure of the traffic network. Despite the methodological differences, the obtained chromatic numbers exhibit a high degree of consistency, indicating the robustness of the proposed framework. Any observed variations can be attributed to the different treatments of uncertainty, indeterminacy, and falsity information within the neutrosophic graph model.

From a traffic management perspective, the comparison demonstrates that all three approaches produce feasible signal phase configurations while accounting for uncertain traffic conflicts. Therefore, the proposed neutrosophic chromatic number framework provides a flexible and reliable tool for traffic-light coordination and signal optimization under uncertain environments.

5.2. Comparison with existing graph-coloring frameworks

To highlight the contribution of the proposed approach, Table 17 presents a qualitative comparison between classical graph coloring, fuzzy graph coloring, intuitionistic fuzzy graph coloring, and the proposed single-valued neutrosophic graph coloring framework.

The proposed framework extends existing graph-coloring approaches by incorporating truth-membership, indeterminacy-membership, and falsity-membership simultaneously. This additional flexibility enables the model to represent uncertain and incomplete traffic-conflict information more effectively than classical, fuzzy, and intuitionistic fuzzy graph-coloring models.

6. Conclusion

This research paper presents a novel framework for determining the neutrosophic chromatic number using α, β, γ-cuts, strong α, β, γ-cuts, independent vertex sets, together with crisp vertex sets and neutrosophic edge sets. The proposed framework extends graph-coloring theory to single-valued neutrosophic graphs by incorporating truth-membership, indeterminacy-membership, and falsity-membership information into the coloring process. Furthermore, theoretical properties of the proposed chromatic numbers are established, including their behavior under union operations of neutrosophic graphs. A comparative analysis of the proposed chromatic-number definitions is also presented to highlight their relationships and to assist in selecting an appropriate approach for different problem settings.

An illustrative traffic-light case study involving three signalized intersections is presented to demonstrate the applicability of the proposed framework. The case study shows how neutrosophic graph coloring can be used to model uncertain traffic conflicts and determine the minimum number of signal phases. For the illustrative network considered, the optimal solution is obtained with five ($k = 5$) signal phases, indicating the potential usefulness of the proposed methodology for organizing compatible traffic movements under uncertainty. The case study is intended solely to illustrate the applicability of the proposed framework and should not be interpreted as a validated traffic-control solution.

The proposed neutrosophic chromatic-number framework provides a flexible mathematical tool for analyzing graph-coloring problems involving uncertainty and indeterminacy, while establishing a foundation for further theoretical developments in neutrosophic graph theory.

A limitation of the illustrative application is that the traffic-flow thresholds and conflict relationships used to construct the neutrosophic membership functions were selected for demonstration purposes rather than being derived from field observations or traffic simulation. Consequently, no validation against real-world traffic data or comparison with existing signal-timing methods has been performed. Future work may investigate data-driven calibration techniques, sensitivity analyses, and validation using real traffic datasets and established traffic simulation models.

As a direction for future research, the proposed chromatic-number concepts may be extended to other classes of neutrosophic graphs, including bipolar neutrosophic graphs, interval-valued neutrosophic graphs, and plithogenic neutrosophic graphs. Further studies may also investigate chromatic numbers under additional graph operations such as product, composition, and join operations. Moreover, the proposed framework has the potential to be applied to broader application domains, including intelligent transportation systems, communication networks, scheduling, resource allocation, and smart-city optimization under uncertain environments, subject to appropriate domain-specific validation.

The computation of neutrosophic chromatic numbers may be further enhanced through the development of optimization algorithms and heuristic techniques. Classical graph-coloring approaches, such as greedy algorithms, branch-and-bound methods, genetic algorithms, particle swarm optimization, simulated annealing, and ant colony optimization, may be extended to neutrosophic graph environments by incorporating truth-membership, indeterminacy-membership, and falsity-membership information into the coloring process. Future research may focus on designing efficient optimization strategies for large-scale neutrosophic graphs and evaluating their performance through comprehensive computational experiments and application-specific validation.

Data availability

No data were used in the research described in this article.

Declaration of competing interest

The authors declare that they have no known competing financial interests or personal relationships that could have appeared to influence the work reported in this manuscript.

Acknowledgment

The authors extend their appreciation to the Deanship of Scientific Research at Northern Border University, Arar, KSA Saudi Arabia, for supporting this work through project number (NBU-FFR-2026-2230-03).

References

[1] L. A. Zadeh, "Fuzzy sets", Information and Control **8** (1965) 338. https://doi.org/10.1016/S0019-9958(65)90241-X.

[2] A. Rosenfeld, "Fuzzy graphs", in Fuzzy sets and their applications to cognitive and decision processes, L. A. Zadeh, K.-S. Fu, K. Tanaka & M. Shimura (Eds.), Academic Press, New York, USA, 1975, pp. 77–95. https://doi.org/10.1016/B978-0-12-775260-0.50008-6.

[3] P. Bhattacharya, "Some remarks on fuzzy graphs", Pattern Recognition Letters **6** (1987) 297. https://doi.org/10.1016/0167-8655(87)90012-2.

[4] J. N. Mordeson & C.-S. Peng, "Operations on fuzzy graphs", Information Sciences **79** (1994) 159. https://doi.org/10.1016/0020-0255(94)90116-3.

[5] I. Rosyida, Widodo, C. R. Indrati & K. A. Sugeng, "A new approach for determining fuzzy chromatic number of fuzzy graph", Journal of Intelligent & Fuzzy Systems **28** (2015) 2331. https://doi.org/10.3233/IFS-141521.

[6] A. Kishore & M. S. Sunitha, "Chromatic number of resultant of fuzzy graphs", Fuzzy Information and Engineering **8** (2016) 229. https://doi.org/10.1016/j.fiae.2016.04.001.

[7] I. Rosyida, Widodo, C. R. Indrati & D. Indriati, "Some properties on fuzzy chromatic number of union of fuzzy graphs through α-cut graphs coloring", Journal of Physics: Conference Series **1306** (2019) 012042. https://doi.org/10.1088/1742-6596/1306/1/012042.

[8] I. Rosyida, Widodo, C. R. Indrati & D. Indriati, "Fuzzy chromatic number of union of fuzzy graphs: An algorithm, properties and its application", Fuzzy Sets and Systems **384** (2020) 115. https://doi.org/10.1016/j.fss.2019.04.028.

[9] R. Mahapatra, S. Samanta & M. Pal, "Applications of edge colouring of fuzzy graphs", Informatica **31** (2020) 313. https://doi.org/10.15388/20-INFOR403.

[10] Z. Gong & J. Zhang, "Chromatic number of fuzzy graphs: Operations, fuzzy graph coloring, and applications", Axioms **11** (2022) 697. https://doi.org/10.3390/axioms11120697.

[11] K. T. Atanassov, "Intuitionistic fuzzy sets", Fuzzy Sets and Systems **20** (1986) 87. https://doi.org/10.1016/S0165-0114(86)80034-3.

[12] K. T. Atanassov, Intuitionistic fuzzy sets: theory and applications, Physica-Verlag, Heidelberg, Germany, 1999. https://doi.org/10.1007/978-3-7908-1870-3.

[13] P. A. Ejegwa, S. O. Akowe, P. M. Otene & J. M. Ikyule, "An overview on intuitionistic fuzzy sets", International Journal of Scientific & Technology Research **3** (2014) 142. https://www.researchgate.net/publication/283120221_An_Overview_on_Intuitionistic_Fuzzy_Sets.

[14] R. Parvathi & M. G. Karunambigai, "Intuitionistic fuzzy graphs", in Computational intelligence, theory and applications, B. Reusch (Ed.), Springer, Berlin, Germany, 2006, pp. 139–150. https://doi.org/10.1007/3-540-34783-6_15.

[15] R. Parvathi, M. G. Karunambigai & K. T. Atanassov, "Operations on intuitionistic fuzzy graphs", IEEE International Conference on Fuzzy Systems, Jeju, Republic of Korea, 2009, pp. 1396–1401. https://doi.org/10.1109/FUZZY.2009.5277067.

[16] M. Akram & B. Davvaz, "Strong intuitionistic fuzzy graphs", Filomat **26** (2012) 177. https://doi.org/10.2298/FIL1201177A.

[17] F. Smarandache, Neutrosophy: Neutrosophic probability, set, and logic: analytic synthesis & synthetic analysis, American Research Press, Rehoboth, NM, USA, 1998.

[18] H. Wang, F. Smarandache, Y. Zhang & R. Sunderraman, "Single-valued neutrosophic sets", Multispace and Multistructure **4** (2010) 410. https://digitalrepository.unm.edu/math_fsp/708.

[19] S. Broumi, M. Talea, A. Bakali & F. Smarandache, "Single-valued neutrosophic graphs", Journal of New Theory **10** (2016) 86. https://doi.org/10.5281/zenodo.50940.

[20] R. Sahin, "An approach to neutrosophic graph theory with applications", Soft Computing **23** (2019) 569. https://doi.org/10.1007/s00500-017-2875-1.

[21] S. Naz, H. Rashmanlou & M. A. Malik, "Operations on single-valued neutrosophic graphs with application", Journal of Intelligent & Fuzzy Systems **32** (2017) 2137. https://doi.org/10.3233/JIFS-161944.

[22] X. Zhang, C. Bo, F. Smarandache & J. Dai, "New inclusion relation of neutrosophic sets with applications and related lattice structure", International Journal of Machine Learning and Cybernetics **9** (2018) 1753. https://doi.org/10.1007/s13042-018-0817-6.

[23] A. Chakraborty, S. P. Mondal, A. Ahmadian, N. Senu, S. Alam & S. Salahshour, "Different forms of triangular neutrosophic numbers, de-neutrosophication techniques, and their applications", Symmetry **10** (2018) 327. https://doi.org/10.3390/sym10080327.

[24] F. Smarandache, "The score, accuracy, and certainty functions determine a total order on the set of neutrosophic triplets (T, I, F)", Neutrosophic Sets and Systems **38** (2020) 1. https://doi.org/10.5281/zenodo.4300354.

[25] M. Kaviyarasu, M. Aslam, F. Afzal, M. Mohammed Saeed, A. Mehmood & S. Gul, "The connectivity indices concept of neutrosophic graph and their application of computer network, highway system and transport network flow", Scientific Reports **14** (2024) 4891. https://doi.org/10.1038/s41598-024-54104-x.

[26] N. Xiang, "Neutrosophic graph theory for evaluation of high-quality party building in driving the high-quality development of universities", Neutrosophic Sets and Systems **86** (2025) 669. https://doi.org/10.5281/zenodo.15514507.

[27] D. Nagarajan, B. Thangavel, Y. Suppiah & K. Anbalagan, "Dynamic neutrosophic decision matrix (DNDM) for smart city", in Data-driven decision making and soft computing: applications and advances, CRC Press, Boca Raton, USA, 2026, pp. 156–173. https://doi.org/10.1201/9781003634836-9.

[28] A. S. Sasipriya & L. Madireddy, "Distance spectrum and energy in single-valued neutrosophic graphs", Neutrosophic Sets and Systems **90** (2025) 343. https://doi.org/10.5281/zenodo.16340798.

[29] J. Muthuerulappan & S. Chelliah, "Exploring edge-neighbor distinguishing proper coloring in neutrosophic graphs: Theory and applications", Journal of Computational Analysis and Applications **33** (2024) 24. https://eudoxuspress.com/index.php/pub/article/view/675.

[30] I. Mary, S. Sandhiya & S. Broumi, "Advancing sustainable mobility: Comparative analysis of MCDM methods with plithogenic and neutrosophic sets", International Journal of Applied Mathematics **38** (2025) 1090. https://doi.org/10.12732/ijam.v38i7s.536.

[31] S. M. Balaji, D. Meiyappan, R. Sujatha & M. Kaviyarasu, "Exploring re-

lationship between neutrosophic topological indices and enhancing chemical reaction pathway optimization through F-index and edge F-index in neutrosophic graphs", Journal of Computational and Applied Mathematics **485** (2026) 117571. https://doi.org/10.1016/j.cam.2026.117571.

[32] A. Syropoulos, B. Papadopoulos & B. K. Sharma, "Neutrosophic graph rewriting as a computational model", in Neutrosophic computing and vague data analysis, Chapman & Hall/CRC, Boca Raton, USA, 2026, pp. 49–63. https://doi.org/10.1201/9781003683339-5.

[33] S. Iftikhar, M. K. Jamil & S. Anwar, "Energy-based neutrosophic fuzzy graphs for cognition-driven organizational decision-making", Cognitive Computation **18** (2026) 70. https://doi.org/10.1007/s12559-026-10603-9.

[34] G. Suriyakumar & V. J. Sudhakar, "The Randi? index in neutrosophic graphs and its applications", Uncertainty Discourse and Applications **3** (2026) 72. https://doi.org/10.48313/uda.vi.71.

[35] A. Jacob, P. B. Ramkumar & P. M. Dhanya, "Directed neutrosophic graph using morphological operators and its applications", Neutrosophic Sets and Systems **96** (2026) 1. https://doi.org/10.5281/zenodo.17096007.

[36] T. Fujita, "Modeling reliability, ambiguity, and risk in information technology management using quaternion fuzzy and quaternion neutrosophic graphs", Journal of Engineering Management and Systems Science (2026) 1. https://www.researchgate.net/publication/406088432.

[37] S. V. Arokia Pratheesha & R. Radha, "A novel approach for the shortest path computation in networks using quadripartitioned single-valued neutrosophic refined numbers", in Neutrosophic computing and vague data analysis, Chapman & Hall/CRC, Boca Raton, USA, 2026, pp. 316–328. https://www.routledge.com/Neutrosophic-Computing-and-Vague-Data-Analysis/Smarandache-Khan/p/book/9781041162025.

[38] F. Karaaslan & B. Davvaz, "Properties of single-valued neutrosophic graphs", Journal of Intelligent & Fuzzy Systems **34** (2018) 57. https://doi.org/10.3233/JIFS-17009.

[39] A. Rohini, M. Venkatachalam, Dafik, S. Broumi & F. Smarandache, "Operations of single-valued neutrosophic coloring", Neutrosophic Sets and Systems **31** (2020) 172. https://fs.unm.edu/nss8/index.php/111/article/view/440.

[40] M. Akram, S. Siddique & B. Davvaz, "New concepts in neutrosophic graphs with application", Journal of Applied Mathematics and Computing **57** (2018) 279. https://doi.org/10.1007/s12190-017-1106-3.

[41] A. Bhaumik, S. K. Roy & D.-F. Li, "(α, β, γ)-cut-set-based ranking approach to solving bi-matrix games in a neutrosophic environment", Soft Computing **25** (2021) 2729. https://doi.org/10.1007/s00500-020-05332-6.

[42] M. Akram & G. Shahzadi, "Operations on single-valued neutrosophic graphs", Journal of Uncertain Systems **11** (2017) 1. https://fs.unm.edu/neut/OperationsOnSingleValued.pdf.

[43] A. Dey & A. Pal, "Vertex coloring of a fuzzy graph using alpha cut", International Journal of Management, IT and Engineering **2**(2012) 340. https://www.academia.edu/download/32564101/IJMRA-MIE1535.pdf.

[44] S. Ismail Mohideen & M. A. Rifayathali, "Coloring of intuitionistic fuzzy graph using (α, β)-cuts", International Research Journal of Mathematics, Engineering and IT **2** (2015) 14. https://www.researchgate.net/publication/334272894_COLORING_OF_INTUITIONISTIC_FUZZY_GRAPH_USING_-CUTS.

[45] M. A. Rifayathali, A. Prasanna & S. Ismail Mohideen, "Intuitionistic fuzzy graph coloring", International Journal of Research and Analytical Reviews **5** (2018) 734. https://www.academia.edu/download/79005754/ijrar_issue_1749.pdf